J. Micropalaeontology, 43, 441–474, 2024
https://doi.org/10.5194/jm-43-441-2024

Journal of Micropalaeontology
Open Access

High Arctic late Paleocene and early Eocene dinoflagellate cysts

Appy Sluijs[1] **and Henk Brinkhuis**[1,2]

[1]Department of Earth Sciences, Laboratory of Palaeobotany and Palynology, Faculty of Geosciences, Utrecht University, 3584 CB Utrecht, the Netherlands
[2]Department of Ocean Systems (OCS), Royal Netherlands Institute for Sea Research (NIOZ), PO Box 1790 AB Den Burg, the Netherlands

Correspondence: Appy Sluijs (a.sluijs@uu.nl)

Received: 27 May 2024 – Revised: 26 August 2024 – Accepted: 5 September 2024 – Published: 8 November 2024

Abstract. Palynomorphs, notably sporomorphs and organic-walled dinoflagellate cysts, or "dinocysts", are the only abundant microfossils consistently present in the sole available central Arctic upper Paleocene to lower Eocene sedimentary succession recovered at the central Lomonosov Ridge by the Integrated Ocean Drilling Program (IODP) Expedition 302 (or the Arctic Coring Expedition, ACEX) in 2004, close to the North Pole. While the analysis and interpretation of a part of these assemblages have so far guided many major stratigraphic, climatological, and paleoenvironmental findings from ACEX, intrinsic details, notably of the dinocyst taxa and assemblages, have not yet been addressed. Here, we present new ACEX dinocyst data for the interval spanning the latest Paleocene to the earliest Eocene (∼ 56.5–53.8 Ma; cores 32X–27X) and integrate these with previous results. We develop a pragmatic taxonomic framework, document critical biostratigraphic events, and propose two new genera (*Guersteinia* and *Sangiorgia*) and seven new species (*Batiacasphaera obohikuenobeae*, *Chaenosphaerula sliwinskae*, *Heterolaucacysta pramparoae, Pyxidinopsis iakovlevae*, *Sangiorgia pospelovae*, *Sangiorgia marretiae*, and *Spiniferella crouchiae*). In addition, we interpret trends and aberrations in dinocyst assemblages in terms of variability in regional temperature, hydrology, and tectonism across the long-term and the Paleocene–Eocene Thermal Maximum (PETM) and Eocene Thermal Maximum 2 (ETM2) global warming phases.

1 Introduction

The partially recovered sedimentary record from the central Lomonosov Ridge, Arctic Ocean (Integrated Ocean Drilling Program (IODP) Expedition 302, or Arctic Coring Expedition (ACEX); Fig. 1) yielded a wealth of new information concerning early Paleogene Arctic paleoclimates, environments, and biogeochemical cycling (Backman et al., 2006). In lower Paleogene sediments overlying an upper Cretaceous unconformity, early work identified the Paleocene–Eocene Thermal Maximum (PETM; ∼ 56 Ma) (Sluijs et al., 2006), the Eocene Thermal Maximum 2 (ETM2; 54 Ma) (Stein et al., 2006; Sluijs et al., 2008b), and the *Azolla* phase (48 Ma; Brinkhuis et al., 2006). These, and many follow-up contributions, revealed that the Arctic was very warm and wet during the early Paleogene, particularly during the PETM and ETM2 (e.g., Willard et al., 2019; Sluijs et al., 2020). Salinities were low throughout, and significant freshening occurred during the PETM, ETM2, and the *Azolla* phase (e.g., Brinkhuis et al., 2006; Pagani et al., 2006; Waddell and Moore, 2008; Sluijs et al., 2009; Speelman et al., 2010; Krishnan et al., 2014). Various papers have also addressed the strong orbital forcing on Arctic temperature and hydrology (Sangiorgi et al., 2008; Sluijs et al., 2008b; Barke et al., 2011; Fokkema et al., 2024b). During the early Paleogene the drill site was apparently located very close to shore, given the large proportions of terrestrial organic matter throughout the record, likely derived from then-exposed parts of the Lomonosov Ridge and Svalbard (e.g., Sluijs et al., 2008b). Often, low-oxygen, euxinic conditions prevailed

at the seafloor, reaching into the lower photic zone during the PETM and ETM2 (e.g., Sluijs et al., 2006, 2009; Stein et al., 2006; März et al., 2011).

Calcareous and siliceous microfossils are typically scarce to absent in this interval, while, in contrast, palynomorphs are abundant and often well preserved (Backman et al., 2006). These particularly comprise pollen and spores derived from terrestrial higher plants and organic-walled dinocysts, besides a suite of other algal remains, organic linings of benthic foraminifera, and acritarchs (Backman et al., 2006). The analysis and interpretation of a part of these assemblages has guided many of the above major stratigraphic, climatological, and paleoenvironmental conclusions. Recent work has assembled and interpreted the pollen and spore record from the latest Paleocene to just above ETM2 with decimeter-scale resolution (cores 32X–27X; Willard et al., 2019). Here, also to aid future Arctic work, we assemble and integrate the unique ACEX dinocyst data for that same interval, integrating new and existing qualitative and quantitative information from analyses carried out previously (Backman et al., 2006, 2008; Sluijs et al., 2006, 2008b, 2009; Fokkema et al., 2024b).

2 Materials and methods

The interval represented by IODP 302 cores 33X to 27X of Hole M0004A straddles the interval from just below the PETM (∼ 56 Ma) to across the ETM2 and possibly the H2 event (54 Ma; Stein et al., 2006; Sluijs et al., 2008b, 2009) (Fig. 2). Recently, Fokkema et al. (2024b) identified eccentricity cycles in the interval immediately below ETM2 and tuned them to two orbital solutions, thereby refining the age model (see Table S1 for age model tie points).

Here, we compile and integrate all existing and new "raw" palynological data underlying the records published so far from cores 33X to 27X of Hole M0004A (Sluijs et al., 2006, 2008b, 2009; Fokkema et al., 2024b) and present them using an existing composite depth scale (Sluijs et al., 2009). All samples were prepared according to the same, typical palynological processing techniques as described in the papers mentioned above. Briefly, after freeze-drying and precision weighing, this involved processing with HCl and HF treatments, followed by sieving residues over a 15 µm mesh sieve. Samples were spiked with a known amount of *Lycopodium clavatum* spores to allow absolute quantitative counts (Stockmarr, 1972). Palynomorphs were counted to a minimum of 200 identifiable dinocysts per sample where possible and to a minimum of 100 identifiable dinoflagellate cysts for the high-resolution palynological investigation in the interval immediately below ETM2. For dinocyst taxonomy, we employ the taxonomy cited in Fensome et al. (2019), except for wetzelielloid taxa, where we follow the recommendations of Bijl et al. (2016). Various consistency checks between the data generated by the two authors (HB and AS), including extensive microscope sessions together and re-counting each other's slides, indicated that counts are consistent at the taxonomical level presented, within an uncertainty of 5 %–10 %. We include a taxonomic section (Sect. 6) that describes selected new taxa and provides an annotated species list. All raw data are provided in the Supplement and on Zenodo (https://doi.org/10.5281/zenodo.10998746, version 4) (Sluijs and Brinkhuis, 2024). A high-resolution version of the Supplement photoplates (38 plates with light microscope photos and 3 plates with scanning electron microscope photos) is also available at Zenodo. All materials are stored in the collection of the Laboratory of Palaeobotany and Palynology, Department of Earth Sciences, Utrecht University, the Netherlands.

3 Results

Palynomorph preservation varies across the section, ranging from (most often) good to poor. The dominant palynological groups throughout the Paleogene ACEX record are dinocysts and the pollen and spores of terrestrial higher plants (Fig. 2). We also recovered many other aquatic algal taxa and acritarchs which were locally quite abundant, sometimes representing up to 30 % of the aquatic palynomorphs. These include *Pterospermella* spp., *Leiosphaera* spp., *Paleotetradinium* spp., *Tasmanites* spp., *Tritonites spinosus*, and *Botryococcus* spp., besides numerous very small (< 20 µm) psilate and skolochorate cysts (viz. "acritarchs"). Organic linings of benthic foraminifera and their fragments are relatively abundant in sediments stratigraphically above and below the PETM (Sluijs et al., 2006), with decreasing abundance up-section. Fungal spores were occasionally encountered as well. In terms of palynofacies, several intervals are dominated by amorphous organic matter (AOM), particularly the upper Paleocene, up to the onset of the PETM, the interval directly overlying the PETM (∼ 381–371 mcd) and the ETM2 interval. Other samples are characterized by a mix of terrestrial plant debris and associated elements. We also regularly encountered pyritized remains of diatoms, Radiolaria, silicoflagellates, and ebridians (Fig. 2).

3.1 Qualitative dinocyst distribution

3.1.1 Peridinioids

Taxonomic issues

Peridinioid cysts with a six-sided ("hexa") second anterior intercalary (para)plate that is involved in archeopyle formation are a major constituent of the assemblages. However, many specimens could not be assigned to a specific or even generic level, either because diagnostic features have not been described, could not be observed, vary from the features described for existing taxa, or could be interpreted as more than one taxon. Specimens present a continuum of morphological characteristics between the descrip-

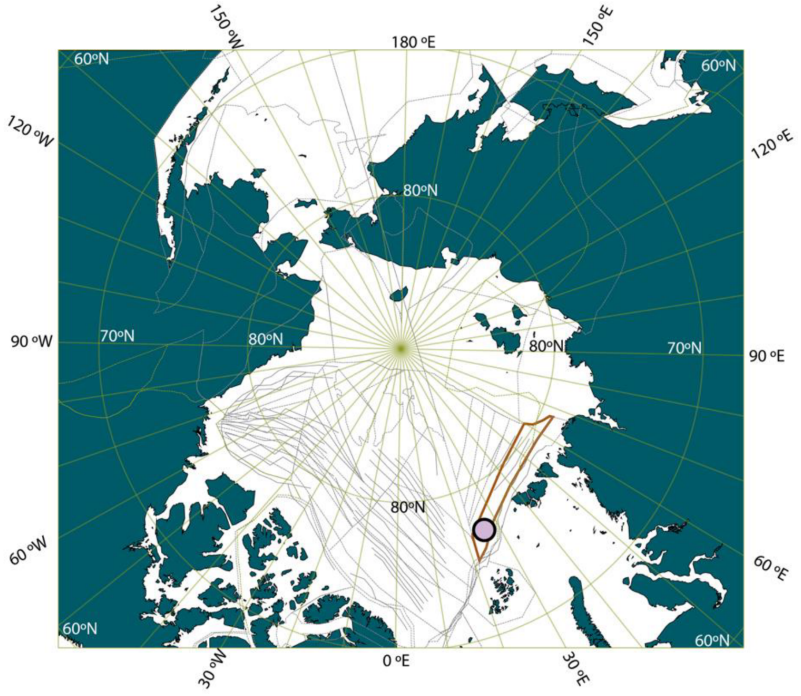

Figure 1. Location of ACEX Hole M0004A on a paleogeographic reconstruction of the Arctic region at the time of the PETM. The reconstruction was made using GPlates (Müller et al., 2018), with the tectonic reconstruction of Seton et al. (2012; the red shape is the Lomonosov Ridge in this reconstruction, and the gray lines are structural features, including spreading ridges) and the paleomagnetic reference frame of Torsvik et al. (2012), and the modern coastlines are indicated.

tions of *Senegalinium*, *Lentinia*, *Spinidinium*, *Cerodinium*, and *Deflandrea*. For example, specimens may range from being "classical" peridinioid-shaped, strongly denticulate with wall striations with steno/isodeltaform 2a archeopyles typical for *Cerodinium*, to faintly striate or smooth with large isodeltaform 2a archeopyles, adhering more to the definition of *Lentinia* and ranging into latideltaform 2a archeopyles as in *Deflandrea*. Other peridinioids may range from being rather small, brown to unpigmented, smooth to granulate cysts without processes, assignable to *Senegalinium*, to specimens with few to numerous spines typical for *Spinidinium*. We noted numerous intermediate morphotypes between these taxonomical entities (see Supplement Plates S8–S13, S34–S36). Preservation is suboptimal in several intervals, which also impacts taxonomical assignments. Future detailed taxonomic work on this group could possibly clarify and complement this work, but we surmise that any evolving concepts will remain challenging to apply. The issues assigning specimens to described taxa primarily arise due to the less detailed taxonomic descriptions that were produced prior to the 1980s.

Taxonomic groupings

Despite the taxonomic ambiguity encountered within the peridinioids with hexa-2a plates, the two authors were in reasonable agreement on the generic level, so counts of *Cerodinium*, *Deflandrea*, *Lentinia*, *Phthanoperidinium*, and *Senegalinium* reflect reliable results. However, we suggest taking abundance percentages of these genera with care and estimate the uncertainty in absolute percentages to be a maximum of 10 %. We decided to group these genera into two broad "complexes" (cpx). We place the recorded variability in the locally highly abundant "morphological continuum" *Cerodinium/Deflandrea/Lentinia* spp. in the *Cerodinium* complex and the *Senegalinium/Spinidinium/Phthanoperidinium* spp. continuum in the *Senegalinium* complex (See Plates S8–S13, S34–S36).

Furthermore, in terms of paleoenvironmental signals, we place both these complexes in a "low-salinity-tolerant group" following previous work (Brinkhuis et al., 2006; Sluijs et al., 2006; Frieling and Sluijs, 2018), in which we also include the few occurring (non-cavate) protoperidinioid dinocysts, such as *Lejeunecysta* spp. and *Selenopemphix* spp. These cysts are known to be derived from heterotrophic species that tolerate low-salinity waters in modern oceans and also indicate regions of high primary production (e.g., Zonneveld et al., 2013). Some taxa within this large category, notably those assignable to the genus *Phthanoperidinium*, are known to be tolerant to lower salinities relative to others (e.g., Liengjarern et al., 1980; Barke et al., 2011), but these are not abundant in this part of the ACEX record. Quadra-2A peridinioids (wetzelielloids) such as *Apectodinium* spp. are not included in

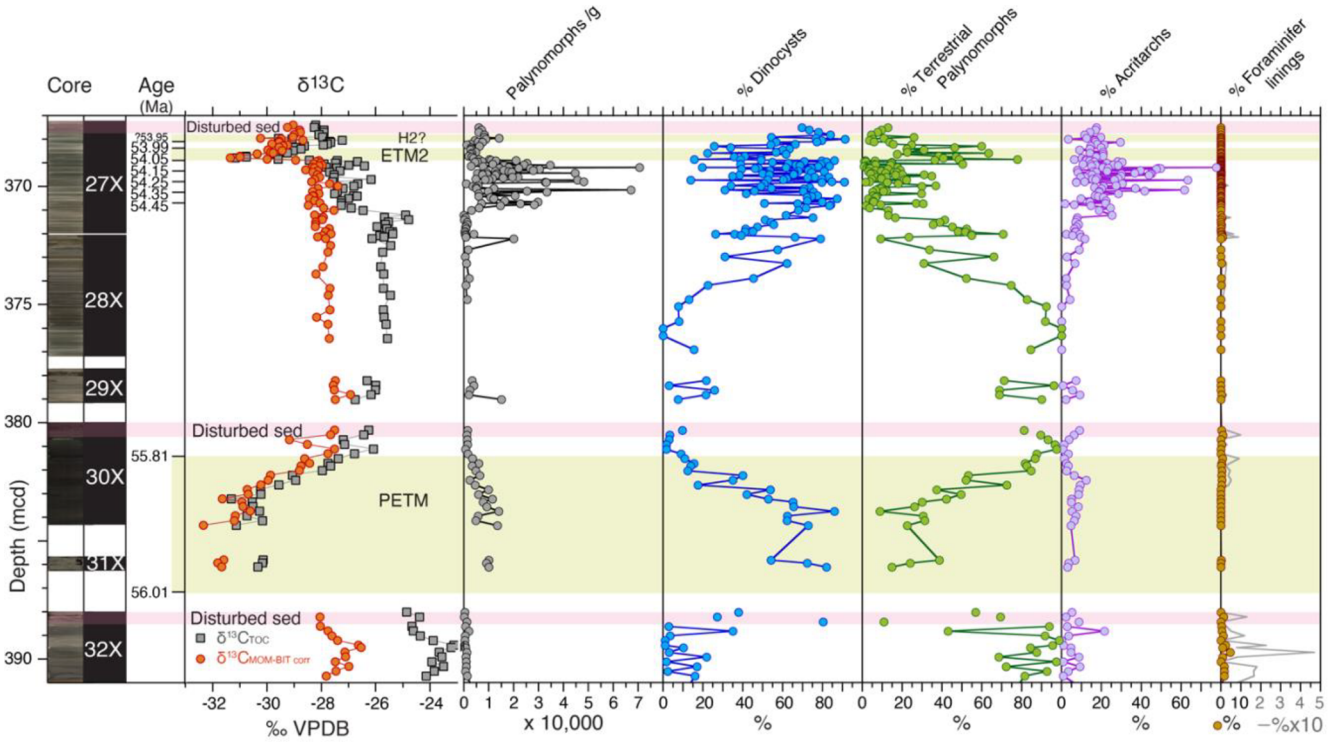

Figure 2. Abundances of major palynological groups across the uppermost Paleocene and lowermost Eocene at ACEX Hole 4A. Core photos and codes (Backman et al., 2006); ages and assignments of PETM, ETM, and H2? (Table S1); and stable carbon isotope records (δ^{13}C) of total organic carbon (TOC), corrected to marine organic matter (MOM) by excluding terrestrial organic matter contributions using the BIT index (see Sluijs and Dickens, 2012), are from cited previous work. Pink bars indicate disturbed sediments, caved from overlying strata during coring. Note the double axis in the column showing the percentage of foraminiferal linings to visualize low abundances.

this group. These taxa appear more indicative of high surface water temperatures on top of a strong tolerance for variable salinities (Bujak and Brinkhuis, 1998; Crouch et al., 2001; Frieling et al., 2014; Frieling and Sluijs, 2018).

3.1.2 Gonyaulacoids

Taxonomic issues

We recorded many gonyaulacoid species that are relatively stable in their morphology and unequivocally assignable to many existing taxa, so that they appear useful for intra-regional to even global correlations with chronostratigraphic value. We also recorded various undescribed taxa with potential paleoecological or stratigraphical value, which were selected for formal description. These include taxa broadly adhering to the "standard building plan" of the cysts of the modern *Gonyaulax spinifera* group, viz. "spiniferitioid" cysts, i.e., sexiform gonyaulacoids with an S-type sulcus, tri- and bifurcated gonal and intergonal processes, that are either isolated or distally connected, like in family member *Nematosphaeropsis*, but differ in having only a part of the processes interconnecting distally with quite pronounced trabeculae. We place these in a new genus, *Sangiorgia*. Based on the size, nature, and shape of the processes, we distinguish two species within this genus, which we name *S. pospelovae* and *S. marretiae*.

Furthermore, we note that some species placed in the genus *Thalassiphora* up to now are morphologically so distinct that there is a need to erect the new genus *Guersteinia* to accommodate standard sexiform gonyaulacoid camocavate cysts with a dorso-ventrally compressed periphragm. We designate the holotype of *Thalassiphora delicata* as the type species of the new genus. Importantly, we note that, by definition, the genus *Thalassiphora* constitutes (typically large) cavate, fibroid gonyaulacoid cysts characterized by dextral torsion and a lack of (para)tabulation. We consider these to be members of the cribroperidinioid lineage of gonyaulacoids that typically exert dextral torsion of the hypocyst relative to the epicyst, which is not the case in *T. delicata* (see also Mudie et al., 2020 for an overview of *Thalassiphora* species and similar deliberations).

In addition, we record an extremely small and psilate new species of *Batiacasphaera*, which we name *B. obohikuenobeae.* Furthermore, we encountered a new taxon lacking an endophragm, assignable to *Chaenosphaerula*, with characteristic, somewhat irregular, tagliatelle-shaped parasutural "bands", which we name *C. sliwinskae*. We also encountered a rather thick-walled species with a microretic-

ulate surface with small irregular outgrowths of low relief assignable to *Pyxidinopsis*, which we name *P. iakovlevae*.

A well-known and long-ranging taxon encountered is *Spiniferella cornuta*. However, these Arctic types are extremely large (consistently > 125 µm in overall length), with the characteristic long, slightly curved apical horn, but are further distinguished here by their rather long gonal processes, which terminate in trifurcate ends that may individually split again into secondary bifurcations or even trifurcations. We describe this as the new species *Spiniferella crouchiae.*

Taxonomic groupings

Despite the relatively large number of morphologically stable taxa discussed above, a major portion of the gonyaulacoids also include morphologically intimately related groups that display formidable intra- and interspecific variation. Following Evitt (1985), these gonyaulacoid representatives within our material include forms assignable to his concepts of the partiforms, the insert and exsert quinqueforms (e.g., goniodomids) and sexiforms and the dorso-ventrally compressed (Gv) insert sexiform (areoligeracean) types, besides those assignable to his categories Gx and Gi (typically including small multi-spined skolochorates).

One of the characteristic features of this interval is the ubiquitous presence of representatives of *Hystrichosphaeridium*, mostly assignable to (subspecies of) *H. tubiferum*. Previous work (e.g., Marheinecke, 1992; Lentin and Williams, 1993; Fauconnier and Masure, 2004; Niechwedowicz, 2022) has also described the enormous morphological variability in this taxon, ranging in shape from "standard" spherical or oval forms to strongly elongated ones (see Plates S20, S21). Additionally, their processes may vary strongly in width and length and in the nature of the distal terminations, where some species form platform-like extensions that can be either perorate or entire. We will refer to this group as the *Hystrichosphaeridium tubiferum* complex.

Morphological variation is also large for the areoligeraceans abundantly recorded here, which represent the dorsoventrally compressed (Gv) gonyaulacoids with an apical archeopyle, like *Areoligera* and *Glaphyrocysta* spp. (cf. Evitt, 1985). Such taxa are typically identified on their process expressions and arrangements, from intra- or penitabular unconnected to complexly interconnected distally, e.g., from *Areoligera coronata* or *A. medusettiformis* types via *Glaphyrocysta ordinata* to *G. exuberans* types. In this material, these morphotypes ("taxa") form a single, fluid complex (see Plates S5–S7) and have therefore been assigned to a single group (the *Areoligera* complex). In effect, our *Areoligera* cpx is identical to that of previous work (Sluijs and Brinkhuis, 2009; Frieling and Sluijs, 2018) and at this location is most often dominated by representatives of *Glaphyrocysta*, notably *G. ordinata*. Among the gonyaulacoids, this group is considered to be characteristic of relatively high-energy, near-shore settings (Brinkhuis, 1994; Sluijs and Brinkhuis, 2009; Harding et al., 2011; Frieling and Sluijs, 2018). However, in the assemblages encountered here, they particularly contrast the large abundances of peridinioids with hexa-2A plates, together with a few other gonyaulacoid groups. As such, together with the other gonyaulacoids, in the present setting, they reflect a normal marine shelf environment, as opposed to a setting with very strong freshwater forcing as indicated by the peridinioids with hexa-2A plates.

We have assigned forms to the (poorly established) genus *Membranosphaera* in previous publications concerning ACEX material (Sluijs et al., 2008b, 2009, 2011; Sluijs and Brinkhuis, 2009) for (mostly) non-tabular holocavate gonyaulacoid cysts with an apical archeopyle. Here we note that the generic name *Elytrocysta* is more suitable for such specimens (Brinkhuis et al., 2003; Williams et al., 2004; Williams et al., 2017) and assign them here accordingly. Morphotypes in this group regularly show vague to clear expression of the paratabulation in their ornamentation. In addition, partly because preservation is not optimal in all samples, it is not always clear if specimens are holocavate or simply consist of an autophragm with numerous (non-)tabular processes. This occasionally abundant category is principally assignable to the partiforms (Evitt, 1985), from *Microdinium* or *Cladopyxidium* types to the morphologically strongly related *Elytrocysta* and *Histiocysta* or *Graptodinium* spp. Consequently, following Sluijs et al. (2008b), the *Elytrocysta* complex consists here of the genera *Elytrocysta*, *Histiocysta/Graptodinium*, and *Microdinium* and intermediates. *Elytrocysta* is by far the dominant genus. The paleoecological significance of the *Elytrocysta* cpx remains rather enigmatic, but cysts in this complex are thought to be derived from open marine, neritic taxa (Frieling and Sluijs, 2018).

Finally, for *Spiniferites* and associated genera, i.e., sexiform gonyaulacoid, S-type sulcus, with gonal processes with typically trifurcate distal ends and possibly intergonal processes with bifurcate distal ends that distally might connect, we use the *Spiniferites* complex, following previous work (e.g., Sluijs et al., 2008a; Sluijs and Brinkhuis, 2009; Harding et al., 2011; Frieling and Sluijs, 2018). In all our samples, the bulk of this group represent *Spiniferites* spp. sensu stricto. This group is typically interpreted to represent marine generalists occurring along the entire inshore-to-offshore transect, relatively abundant in warm open marine settings in the modern period (Wall et al., 1977; Thöle et al., 2023) and in the Eocene (Brinkhuis, 1994; Frieling and Sluijs, 2018).

Biostratigraphy

Among both existing and new species, we recorded several empirically established stratigraphically important taxa that can be used for interregional correlations, besides the potentially useful first occurrences (FOs) among the new species (Fig. 3). We treat them chronologically in this section. The calculated ages of these events, using simple linear interpo-

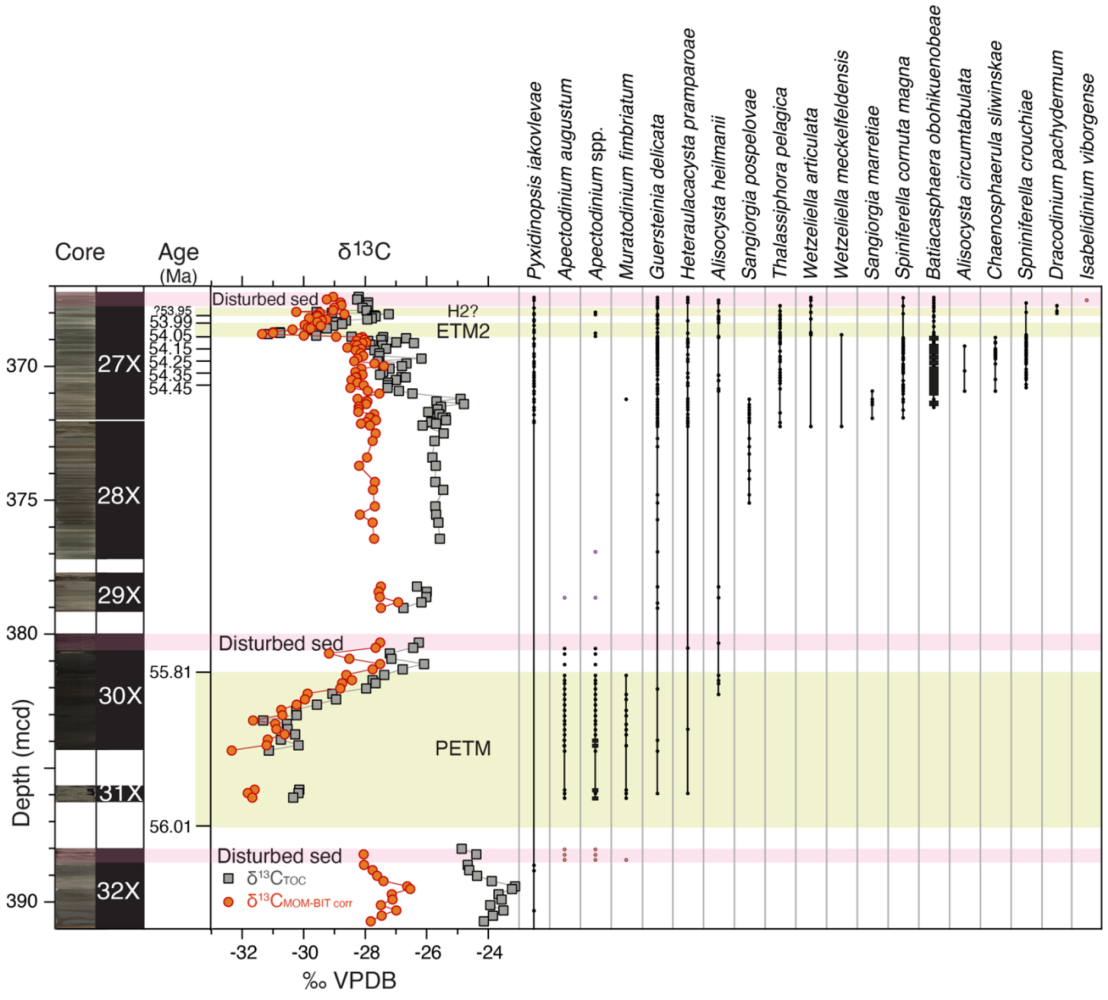

Figure 3. Range chart of (potentially) stratigraphically useful first and last (consistent) dinocyst occurrences and the newly described taxa across the uppermost Paleocene and lowermost Eocene at ACEX Hole 4A. Core photos and codes (Backman et al., 2006); ages and assignments of PETM, ETM and H2? (Table S1); and stable carbon isotope records ($\delta^{13}C$) of total organic carbon (TOC), corrected to marine organic matter (MOM) by excluding terrestrial organic matter contributions using the BIT index (see Sluijs and Dickens, 2012), are from cited previous work. Pink bars indicate disturbed sediments, caved from overlying strata during coring. Occurrences shown in orange in these intervals are assumed to reflect downcore contamination due to caving (see text).

lations between the tie points of our age model using ages of 56.0 and 54.0 for the onsets of the PETM and ETM2, respectively, are presented in Table 1.

Cerodinium wardenense occurs throughout the record and is therefore not shown in Fig. 3. The last occurrence of *C. wardenense* in the North Sea closely coincides with the top of the *H. tubiferum* zone of Bujak and Mudge (1994), which is close to calcareous nannofossil zone boundary NP10–NP11. Based on this, the presence of *C. wardenense* within the carbon isotope excursion (CIE) at ∼ 369 mcd, first identified by Stein et al. (2006), confirmed this CIE to represent ETM2 (Sluijs et al., 2008b). The new species *Pyxidinopsis iakovlevae* ranges throughout the studied interval but notably in the upper Paleocene and the interval below ETM2.

Apectodinium augustum, the total range of which is diagnostic for the PETM interval, first occurs in the uppermost 0.5 m of Core 32X, but this interval represents caved sediments from overlying strata. The first in situ occurrence is hence in Core 31X, representing a first occurrence in the core gap at 387.36 (±1.26) mcd, consistent with the onset of the PETM and its carbon isotope excursion (Sluijs et al., 2006). The last consistent occurrence is at 381.41 (±0.1) mcd, which marks the top of the CIE. Isolated specimens recorded above this level might be reworked due to sea level regression after the PETM (Sluijs et al., 2008a, b). The range of *A. augustum* is approximately consistent with the oldest *Apectodinium* acme, which is recorded globally during the PETM and – in combination – typically restricted to the CIE (Crouch et al., 2001; Frieling and Sluijs, 2018; Denison,

Table 1. Stratigraphic constraints on recognized dinocyst events (Fig. 3) and their calculated ages. Ages are determined using simple linear interpolations between the tie points of our age model using the ages of 56.0 and 54.0 for the onsets of the PETM and ETM2, respectively, and tuned eccentricity maxima (see Table S1). LO: last occurrence. FO: first occurrence. LCO: last common occurrence.

Biostratigraphic datum		Upper depth limit						Lower depth limit						
		Core	Section	cm (top)	cm (bottom)	Sample depth average (mcd)	Sample age (ka)	Core	Section	cm (top)	cm (bottom)	Sample depth average (mcd)	Sample age (ka)	Event age (ka)
FO	*Dracodinium pachydermum*	27X	1	59	61	368.000	53 951	27X	1	64	66	368.050	53 958	53 955
FO	*Chaenosphaerula sliwinskae*	27X	3	6	7	370.465	54 398	27X	3	10	12	370.510	54 406	54 402
LO	*Sangiorgia marretiae*	27X	3	40	42	370.810	54 454	27X	3	50	52	370.910	54 467	54 460
FO	*Alisocysta circumtabulata*	27X	3	50	52	370.910	54 467	27X	3	60	62	371.010	54 479	54 473
LO	*Sangiorgia pospelovae*	27X	3	60	62	371.010	54 479	27X	3	80	82	371.210	54 505	54 492
FO	*Batiacasphaera obohikuenobeae*	27X	3	110	112	371.510	54 543	27X	3	120	122	371.610	54 556	54 550
FO	*Spiniferella crouchiae*	27X	3	150	151	371.905	54 594	27X	4	0	2	371.920	54 596	54 595
FO	*Sangiorgia marretiae*	27X	3	150	151	371.905	54 594	27X	4	0	2	371.920	54 596	54 595
FO	*Thalassiphora pelagica*	27X	CC			372.220	54 634	28X	1	40	42	372.680	54 693	54 664
FO	*Wetzeliella meckelfeldensis*	27X	CC			372.220	54 634	28X	1	40	42	372.680	54 693	54 664
FO	*Wetzeliella articulata*	27X	CC			372.220	54 634	28X	1	40	42	372.680	54 693	54 664
FO	*Sangiorgia pospelovae*	28X	2	130	132	375.080	55 000	28X	3	40	42	375.710	55 081	55 040
LCO	*Apectodinium augustum*	30X	1	101	103	381.320	55 798	30X	1	121	123	381.520	55 814	55 806
LO	*Muratodinium fimbriatum*	30X	1	101	103	381.320	55 798	30X	1	121	123	381.520	55 814	55 806
FO	*Heteraulacacysta pramparoae*	31X	CC	23	25	385.940	55 976	31X	CC	40	42	386.110	55 983	55 980
FO	*Apectodinium augustum*	31X	CC	40	42	386.110	55 983	32X	1	61	63	388.620	56 157	56 010
FO	*Muratodinium fimbriatum*	31X	CC	40	42	386.110	55 983	32X	1	61	63	388.620	56 157	56 010

2021), although it leads the CIE in several records by millennia (Sluijs et al., 2007; Jin et al., 2022). The expression of the *Apectodinium* acme at the central Lomonosov Ridge is less extreme than in other records around the globe (Bujak and Brinkhuis, 1998; Crouch et al., 2001; Sluijs and Brinkhuis, 2009; Sluijs et al., 2011; Kender et al., 2012; Denison, 2021), with maximum percentages of $\sim$ 20. However, these percentages are still diagnostic of the PETM in this section. The drill site seems outside the geographic (or temperature?) range of *Apectodinium* spp. for the remainder of the studied interval, except for a brief return in two samples at the onset of ETM2 (368.84–368.72 $\pm$0.02 mcd, not *A. augustum*), corroborating its poleward spread during global warming phases (Bujak and Brinkhuis, 1998; Sluijs et al., 2009). Given the dominance of low-salinity-tolerant dinocysts, we surmise that representatives of *Apectodinium* were outcompeted due to low salinity and lower temperatures, but it is possible that the genus was more abundant in the Arctic in less proximal/more saline settings during the PETM and ETM2. Interestingly, some specimens of multiple *Apectodinium* species are remarkably small.

Partly consistent with the stratigraphic distribution of *Apectodinium* spp. is the occurrence of *Muratodinium fimbriatum* (Fig. 3). The effective range of this species is restricted to the PETM, apart from a single specimen at 371.20 rm b.s.f. This FO seems consistent with that in various Nordic Sea locations, including the Labrador Sea (Nøhr-Hansen et al., 2016), the North Sea (Powell et al., 1996), and the Turgay Strait (Iakovleva et al., 2001), but this taxon ranges slightly deeper down into the Paleocene at lower-latitude sites, such as the New Jersey shelf (Sluijs and Brinkhuis, 2009) and South Carolina (Edwards, 1998) in the USA, various locations along Tethys margins (Henk Brinkhuis, personal observations, 1985–2025), the eastern equatorial Atlantic Ocean (Frieling et al., 2018b), and India (Prasad et al., 2020), and was originally described from strata close to the PETM (Frieling et al., 2018a) by Cookson and Eisenack (1967). It seems that this species is one of many that shows poleward migration during the PETM (see overview of Frieling and Sluijs, 2018). We do note the conspicuous absence of the morphologically related species, *Ifecysta pachyderma*, which, at low and mid-latitudes, is typically found in tandem with *M. fimbriatum*. Empirical evidence suggests that the former was essentially a true tropical variety of this cribroperidinioid group.

Alisocysta heilmannii and the new species *Heteraulacacysta pramparoae* first occur within PETM strata, but their presence is sporadic. Given the rarity of dinocysts below the PETM, we cannot exclude that these taxa were already present in the region during the Paleocene. The species range throughout the entire studied interval. For *A. heilmanii*, this is consistent with its range in the North Sea (Heilmann-Clausen, 1985; Casas-Gallego et al., 2021).

The FO of the genus *Sangiorgia* is represented by the FO of *S. pospelovae* at 375.40 (±0.31) rm b.s.f., but we have recorded several specimens in the underlying samples that resemble this species. The last occurrence is at 371.11 (±0.05) rm b.s.f.

Several FOs are concentrated near the base of Core 27X, likely implying an FO in the core gap between the top of undisturbed sediments in Core 28X (372.68 rm b.s.f.) and the bottom of Core 27X (372.22 rm b.s.f.). This includes the FO of *Thalassiphora pelagica*. This interval is also the base of the very short range of *Sangiorgia marretiae* between 371.97 (±0.05) and 370.86 (±0.05) rm b.s.f. The FOs of *Wetzeliella articulata* and *W. meckelfeldensis* are also in this interval, and another useful event among the wetzelielloids includes the FO of *Dracodinium pachydermum* in Core 27X at 360.02 (±0.03) rm b.s.f. The FOs of these wetzelielloids appear internally consistent with the succession as recorded in the North Sea, Shetland, and Norwegian basins (e.g., Bujak and Mudge, 1994).

Slightly higher up, we detect the FO of *Batiacasphaera obohikuenobeae* at 371.56 (±0.05) rm b.s.f., after which it rapidly becomes an abundant constituent and dominates assemblages up to the onset of ETM2. The species reappears after ETM2 and ranges up to the top of the studied section, including the upper part that represents caved material, suggesting its range exceeds the studied time interval. In this interval, we also record sporadic *Alisocysta circumtabulata*, much later than in the North Sea (e.g., Powell et al., 1996). At the same level, we record the first indisputable occurrence of *Chaenosphaerula sliwinskae* at 369.88 rm b.s.f., but a few cysts resembling this new species were recorded down to 370.9 rm b.s.f. It is never an abundant species, and its occurrence is somewhat scarce up to its LO at 368.89 (±0.01) rm b.s.f. Closely above this FO, we record the FO of the new species *Spiniferella crouchiae*, which ranges at least to the top of the study interval.

In addition, and somewhat remarkably, we have recorded a single specimen of *Isabelidinium viborgense* in the top interval of Core 27X, which likely represents caved material. This is a stratigraphic index taxon for the Selandian (e.g., Heilmann-Clausen, 1985; Vieira et al., 2020), which is not present in the ACEX material due to a significant hiatus between the Cretaceous and the late Paleocene (Backman et al., 2006). We therefore conclude that the Selandian was once deposited close to, and presumably at, the drill site, eroded during the early Eocene leading to its reworking, and was subsequently redeposited in caved sediments on top of Core 27X. We surmise it is present in the poorly recovered ∼ 60 m overlying the studied interval.

3.2 Quantitative dinocyst distribution patterns

3.2.1 Dinocyst paleoecological framework

As indicated above, for our quantitative description of the assemblages, we make effective taxonomic and ecological dinocyst groups derived from modern distributions (e.g., Zonneveld et al., 2013; Thöle et al., 2023) and empirically based paleoecological information of Paleogene dinocysts following previous work (e.g., Brinkhuis, 1994; Powell et al., 1996; Brinkhuis et al., 1998; Pross and Schmiedl, 2002; Crouch and Brinkhuis, 2005; Pross and Brinkhuis, 2005; Sluijs et al., 2005; Eldrett and Harding, 2009; Harding et al., 2011; Frieling and Sluijs, 2018; Vieira and Jolley, 2020; Bijl et al., 2021a; Iakovleva and Heilmann-Clausen, 2021; Jolley et al., 2023). Moreover, we generally follow the quantitative empirical framework of Sluijs and Brinkhuis (2009) and Frieling and Sluijs (2018). Assignment of species to ecogroups is specified in Sect. 6.2.

3.2.2 Dinocyst distribution patterns

Dinocyst assemblages in the uppermost Paleocene (Core 32X), several intervals between the PETM and ETM2, notably the uppermost 1 m of Core 30X, parts of Core 29X, and the lowermost 2 m of Core 28X, are very low in diversity and are dominated by representatives of the hexa-2A peridinioid *Senegalinium* cpx and *Cerodinium* cpx with minor contributions from the gonyaulacoid *Spiniferites* spp. and

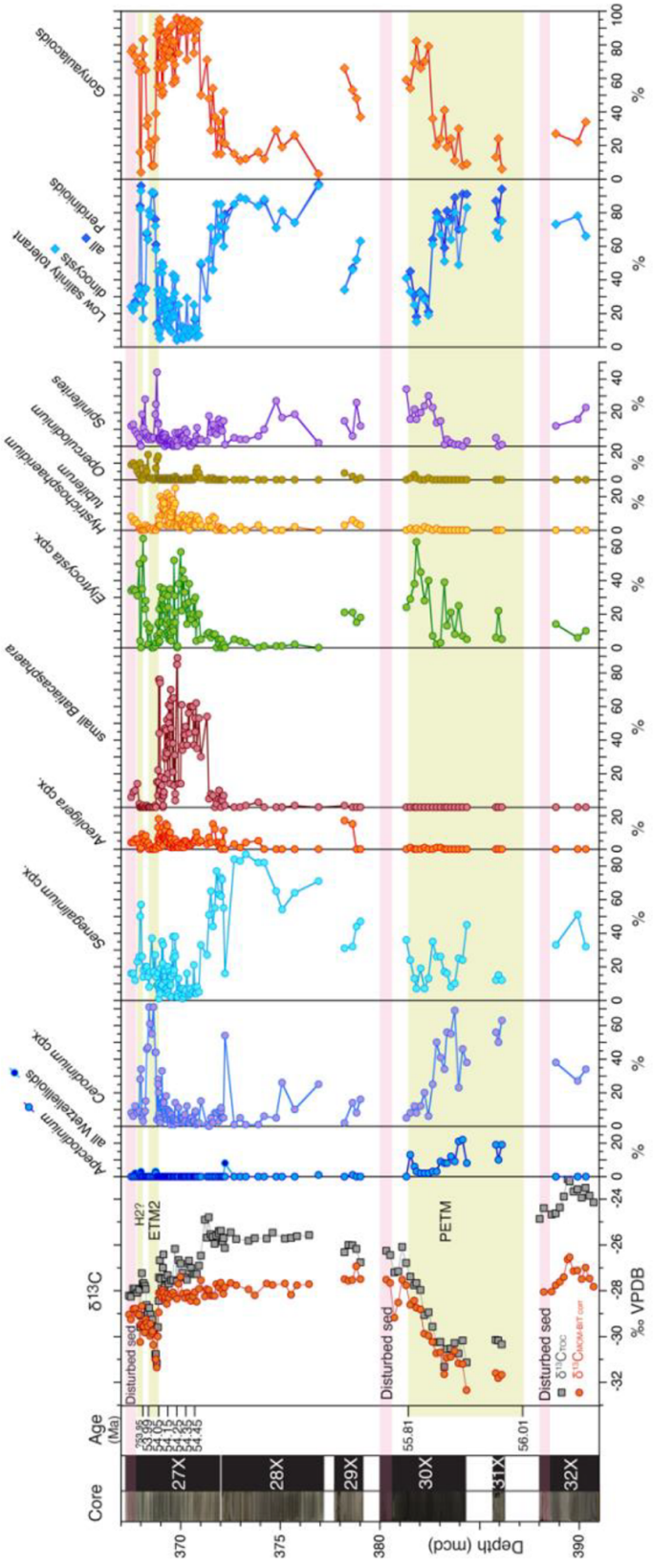

Figure 4. Dinocyst (group) abundances across the uppermost Paleocene and lowermost Eocene at ACEX Hole 4A. Core photos and codes (Backman et al., 2006); ages and assignments of PETM, ETM, and H2? (Table S1); and stable carbon isotope records ($\delta^{13}C$) of total organic carbon (TOC), corrected to marine organic matter (MOM) by excluding terrestrial organic matter contributions using the BIT index (see Sluijs and Dickens, 2012), are from cited previous work. Pink bars indicate disturbed sediments, caved from overlying strata during coring.

the *Elytrocysta* cpx (Fig. 4). Palynological assemblages in these intervals are overwhelmingly dominated by terrestrial palynomorphs (Fig. 2). Dominant amorphous organic matter (AOM) is considered to be of terrestrial origin given the dominance of other terrestrial components such as cuticles and pollen. Marine components are so rare that dinocyst assemblages are unquantifiable in many samples. During both the PETM and ETM2, the *Cerodinium* cpx dominates assemblages, also with abundant *Apectodinium* spp. in the PETM interval. Dinocyst taxonomic diversity is also much greater during the PETM.

We find much more diversity among gonyaulacoids, notably *B. obohikuenobeae*, the *Elytrocysta* cpx, the *Areoligera* cpx, and the *Hystrichosphaeridium tubiferum* cpx, besides *Operculodinium* spp. and *Spiniferites* spp., in the interval between 371.35 (±0.05) mcd and the onset of ETM2. This interval represents the time during which the drill site was located most distally from the coast in the Paleogene section of the ACEX record, suggesting a relation between abundance and relative sea level (Sluijs et al., 2009; Fokkema et al., 2024b). Indeed, small *Batiacasphaera* cysts, such as *B. obohikuenobeae*, are typically characteristic of open-ocean conditions throughout the Cenozoic (e.g., Schreck et al., 2013). Together with the other gonyaulacoid species, we therefore consider their paleoecology as "open marine", thereby contrasting them to the low-salinity-tolerant group.

Although members of the *Cordosphaeridium fibrospinosum* complex (Brinkhuis and Schiøler, 1996; Sluijs and Brinkhuis, 2009; Frieling and Sluijs, 2018) are present in the studied material, they never dominate assemblages. Similarly, we encounter some Goniodomidae with an epicystal archeopyle, notably *Eocladopyxis*, *Heteraulacacysta*, and *Polysphaeridium*, but never as a significant component of the assemblage. This contrasts with records from time-equivalent locations globally (e.g., Crouch and Brinkhuis, 2005; Sluijs and Brinkhuis, 2009; Sluijs et al., 2011; Frieling et al., 2018b) and suggests that environmental conditions, perhaps temperature, light regime, and salinity, were not optimal for these groups.

4 Discussion

4.1 Hydrological change, sea level rise, and eutrophication during the PETM

Previous work has already described (1) the terrestrially dominated latest Paleocene with a dominance of cysts derived from low-salinity-tolerant dinoflagellates, (2) the change to a more open marine palynological assemblage but with the persistence of the low-salinity-tolerant taxa during the PETM, and (3) the first abundances of various "open marine" gonyaulacoid taxa in its aftermath (Sluijs et al., 2006, 2008b). These three phases imply a change from a very proximal position of the drill site relative to the coast with limited marine influence during the late Paleocene to a more offshore position during the PETM due to sea level rise but with persistently low salinities due to the invigorated hydrological cycle. The incursion of "open marine" gonyaulacoid taxa during the recovery of the PETM suggests an increase in salinity but a still higher relative sea level. Above the PETM, palynological assemblages are again dominated by terrestrial material, suggesting a sea level return to the late Paleocene situation.

We note that dominant *Senegalinium* cpx prior to the PETM is replaced by dominant *Cerodinium* cpx during the PETM (Fig. 4), notably by *Cerodinium* spp. Both of these genera and complexes are considered to be produced by dinoflagellates that were tolerant to low salinities and preferred relatively nutrient-rich environments, and they are typically treated as a single paleoecological group termed hexa-2A peridinioids or *Senegalinium* complex (Frieling and Sluijs, 2018, and references therein). Previously, a distinction within this larger group was made regarding the degree of tolerance to low salinities, with species of *Phthanoperidinium* being more tolerant than *Senegalinium* based on patterns recorded in the *Azolla* phase at the Lomonosov Ridge, when the sea surface became (intermittently) fresh (Barke et al., 2011). Analogously, it is possible that a shift towards lower salinities benefited representatives of *Cerodinium* more than *Senegalinium* spp., but, given the abundances of *Senegalinium* spp. during the *Azolla* interval (Barke et al., 2011) and much lower abundances of specimens of *Cerodinium*, this seems unlikely. Similarly, given the cosmopolitan distribution of both taxa, we do not surmise a strong influence of PETM warming on their relative abundances. Rather, we surmise that representatives of *Cerodinium* were able to benefit more than their *Senegalinium* counterparts from sea surface eutrophication following more intense food and nutrient supply from land during the PETM (e.g., Sluijs et al., 2008b), or the two groups were targeting other food sources or types.

Supporting evidence for these hydrological and productivity changes during the PETM comes from hydrogen isotope records of higher-plant n-alkanes (Pagani et al., 2006), a vast increase in sediment accumulation rates (Sluijs et al., 2008b), TOC enrichments (Sluijs et al., 2006; Stein et al., 2006), and ample evidence for water-column and seafloor deoxygenation resulting from this hydrological change, warming, and eutrophication (Sluijs et al., 2006, 2008b; März et al., 2010).

4.2 Sea level change between the PETM and ETM2

In strata overlying the PETM, palynological associations are dominated by terrestrial material and palynomorphs, and dinocysts are often too diluted to quantify assemblages, particularly in the upper part of Core 30X and the lower part of Core 28X (Fig. 2). The dominance of *Cerodinium* cpx and *Senegalinium* cpx (Fig. 4), cysts derived from low-salinity-tolerant dinoflagellates, confirms a setting proximal to the coastline. The drill site was located somewhat more distally during the deposition of sediments recovered in Core 29X.

In the lower 1 m of Core 27X, the interval between ∼ 54.7 and 54.5 Ma, gonyaulacoid taxa become increasingly abundant (Fig. 4) and the dominance of terrestrial palynomorphs is gradually replaced by marine palynomorphs (Fig. 2), suggesting an increasingly distal position of the drill site relative to the coast. This is consistent with a previously recorded rise in sea level (Fokkema et al., 2024b). While sediments below this transgressive surface were likely deposited just below wave base, given the lack of marine indicators, the overlying interval represents the most distal setting of the study interval and biomarker assemblages suggest water depths of significantly more than 200 m (Fokkema et al., 2024b). Transgression is also supported by the high glauconite content of the sediments. Glauconite formation requires formation of thousands of years at the sediment–water interface (Prothero and Schwab, 2004). The associated sediment starvation is interpreted to reflect shoreward migration of sedimentation.

4.3 Cosmopolitanism among early Eocene dinocyst taxa

The relatively diverse, open marine assemblages between 371–369 mcd (54.5–54.0 Ma) are not only unique for the upper Paleocene–lower Eocene section, but also in the broader context of Paleogene dinocyst assemblages in the ACEX record, which are typically dominated by hexa-2A peridinioids (Sangiorgi et al., 2008; Sluijs et al., 2008b; Barke et al., 2011). The latter are still abundant in a few samples but typically comprise between 5 % and 20 % of the assemblage, with higher values in only a few samples. Gonyaulacoid taxa, typically *B. obohikuenobeae* and sometimes *Elytrocysta* spp., usually dominate assemblages. Moreover, *Spiniferites* spp., *Glaphyrocysta ornata* (*Areoligera* cpx.), and *Hystrichosphaeridium tubiferum* cpx are common in almost all samples, as are regular abundances of *Operculodinium* spp.

Abundances of *Spiniferites* spp., *Areoligera* cpx, *Elytrocysta* spp., and *Hystrichosphaeridium tubiferum* cpx are common in numerous early Eocene mid- to high-latitude sites of the Northern (Powell et al., 1996; Iakovleva et al., 2001; Eldrett and Harding, 2009; Sluijs and Brinkhuis, 2009; Rush et al., 2023) and Southern hemispheres (Crouch et al., 2020; Bijl et al., 2021a, b; Premaor et al., 2023). Many of these aspects, notably representatives of *Spiniferites* cpx, *Operculodinium* spp., and *Areoligera* cpx, are common to abundant constituents in low-latitude regions as well (Gregory and Hart, 1995; Crouch et al., 2003; Frieling et al., 2018b; Steeman et al., 2020). This confirms that the taxa recorded in this section, including the hexa-2A peridinioids, were truly cosmopolitan, inhabiting shallow marine settings from the Antarctic shelf to the Lomonosov Ridge. The occurrence of truly global distributions in any dinocyst in geological time is remarkable given the strong meridional biogeographic separation of dinocyst taxa in the modern period (Zonneveld et al., 2013). The global occurrence of so many taxa that often dominate assemblages worldwide during the early Eocene implies that the extremely low temperature gradients in this time period (Huber and Caballero, 2011; Cramwinckel et al., 2018; Hollis et al., 2019; Fokkema et al., 2024) were likely associated with low global meridional marine biodiversity gradients and that temperature may not have been the dominant forcing of marine biogeographic patterns, in contrast to the present day.

4.4 ETM2

Previous work on ETM2 already indicated a vast drop in sea surface salinity, as indicated by the loss of normal marine taxa, the dominance of the low-salinity-tolerant group, and an increase in the supply of terrestrial pollen and spores through increased run-off (Fig. 3, Sluijs et al., 2009). The recent insight that the water depth of the drill site significantly exceeded 200 m during this phase (Fokkema et al., 2024b), which must have also increased the distance of the site to the coastline, makes this response even more remarkable. It not only suggests that run-off increased in coastal areas, but also that larger areas of the surface ocean, even those located somewhat more distally, were insufficiently salty for normal marine dinoflagellates to thrive.

Like the PETM, the largest abundance increase during ETM2 was in numbers of representatives of the *Cerodinium* cpx. Analogous to the PETM (see Sect. 4.1), this may have resulted from an increased supply of food and nutrients from land through intensified run-off. The abundance of amorphous organic matter and TOC enrichments within ETM2 is consistent with this interpretation, although this is likely a combined effect of supply and enhanced preservation due to the development of anoxic conditions at the seafloor and in the water column (Stein et al., 2006; Sluijs et al., 2009).

5 Conclusions

We develop a pragmatic taxonomy and paleoecological grouping of late Paleocene–early Eocene dinoflagellate cysts encountered in sediments recovered during the IODP ACEX expedition on the Lomonosov Ridge, Arctic Ocean, representing the first and only (academic) Arctic record for this time interval. We describe two new dinocyst genera and six new species. We record several first occurrences of species, including several new ones, which may have value for regional or global biostratigraphic correlations.

Strong variations in the relative abundance of terrestrial and marine palynomorphs show evidence of sea level variability, notably related to eustatic rise during the PETM at ∼ 56 Ma, and a likely much larger, likely tectonic-forced sea level rise at ∼ 54.5 Ma. Both during the PETM and ETM2, we record the influx of thermophilic species into the Arctic region, notably *Apectodinium*, *Muratodinium fimbriatum*, and also several other wetzelielloids during ETM2. The events are further marked by strong freshwater forcing, as indicated by freshwater-tolerant taxa peridinioid dinoflagel-

lates. We suggest that the notable increase in *Cerodinium* spp. within this freshwater-tolerant group may be related to eutrophication.

We also note that components of the dinocyst assemblages are identical to those at the adjacent Nordic seas, the mid-latitudes, and the tropics all the way to the Southern Ocean. The global occurrence of so many taxa that often dominate assemblages worldwide during the early Eocene implies that the extremely low meridional temperature gradients during this time period were likely associated with low global meridional marine biodiversity gradients. In contrast to the modern period, temperature may not have been the dominant forcing of marine biogeographic patterns.

6 Taxonomy

We formally describe the new genera and species in Sect. 6.1, of which photographs of holotypes and paratypes are presented in Sect. 6.2. Section 6.3 includes a complete species list with remarks and taxonomical and ecological grouping, supported by an extensive collection of photographs in the Supplement (low-resolution version; high resolution available at Zenodo (Sluijs and Brinkhuis, 2024, version 4: https://doi.org/10.5281/zenodo.10998746).

6.1 Systematic paleontology

Division Dinoflagellata (Bütschli, 1885; Fensome et al., 1993)

Class Dinophyceae (Pascher, 1914)

Subclass Peridiniphycidae (Fensome et al., 1993)

Order Gonyaulacales (Taylor, 1980)

Suborder uncertain

Family uncertain

Genus *Batiacasphaera* (Drugg, 1970; emend. Morgan, 1975)

Batiacasphaera obohikuenobeae sp. nov.
Plates 1, S3, S4, S39

Derivation of name. Named for Francisca Oboh-Ikuenobe, in recognition of her achievements in marine palynology, Missouri State University of Science and Technology, Rolla, Missouri, USA.

Diagnosis. A small, spherical, and thin-walled gonyaulacoid cyst with an autophragm only. The cyst surface appears completely smooth to psilate, to incidentally microgranulate under light microscopy. SEM analyses show a micrometer-scale reticulate surface (see Plate S39). Tabulation is only apparent from the archeopyle, which is formed by the release of all the apical paraplates (tA, compound) and is distinctly angular. The paraplates reflecting 2' and 3' are much larger than 1' and 4'. The operculum is usually detached, but sometimes plate 1' remains attached to the anterior sulcal plate.

Holotype. Plate 1, A–C

Paratypes. Plate 1, D–F, G–H

Material. IODP 302 Hole M0004A, Lomonosov Ridge, Arctic Ocean

Type locality and horizon. IODP 302 Hole M0004A, Lomonosov Ridge, Arctic Ocean, lower Eocene Core 302-0004A-27X-03-04 cm.

Age. Early Eocene

Description.

Shape: (sub)spherical.

Wall relationships: autophragm only.

Wall features: appears completely smooth to psilate, to incidentally microgranulate under light microscopy. SEM analyses show a micrometer-scale reticulate surface.

Processes: absent.

Paratabulation: indicated by archeopyle only.

Archeopyle: formed by the release of all the apical paraplates (tA, compound); distinctly angular. The paraplates reflecting 2' and 3' are much larger than 1' and 4'. The operculum is usually detached, but sometimes plate 1' remains attached to the anterior sulcal plate.

Paracingulum: indeterminable.

Parasulcus: indeterminable.

Dimensions. Diameter 18–25 µm ($n = 10$).

Holotype. 22 µm.

Paratypes. 23 µm.

Stratigraphic range/occurrence. Early Eocene

Remarks. In our material, we locally encountered numerous small, round, thin-walled, colorless, psilate to microgranulate gonyaulacoid cysts with an apical archeopyle, which must be included in the genus *Batiacasphaera*. Using light microscopy, the apical archeopyle is often folded in such a way that it strongly resembled a Type 3I, but SEM micrography confirmed type TA. The species resembles representatives of *Batiacasphaera* often encountered in Neogene open-ocean sediments, such as *B. micropapillata*, *B. minuta*, and *B. sphaerica*, but it differs in its extremely small size and its general lack of ornamentation when viewed using light microscopy.

Genus *Pyxidinopsis* (Habib, 1975; emend. Stover and Evitt, 1978)

Pyxidinopsis iakovlevae sp. nov.
Plates 5, 6, S25, 26, 27

Derivation of name. Named for Alina I. Iakovleva, in recognition of her achievements in marine palynology, at the Geological Institute, Russian Academy of Sciences, Moscow, Russian Federation

Diagnosis. A species of *Pyxidinopsis*, intermediate in size, with a relatively thick, punctate to most often microreticulate surface, characterized by frequent small, solid, irregularly

shaped and distributed rod-like features. No other surface ornamentation present. Archeopyle relatively large, precingular, type P (3″ only); operculum free. Paratabulation indicated by archeopyle only. No traces of paracingulum or parasulcus.

Holotype. Plate 6, A–C

Paratypes. Plate 5, A–C, D–E, F–H; Plate 6, D–E, F–G

Material. IODP 302 Hole M0004A, Lomonosov Ridge, Arctic Ocean

Type locality and horizon. IODP 302 Hole M0004A, Lomonosov Ridge, Arctic Ocean, upper Eocene, sample 302-4A-27X-3-20/22

Age. Late Paleocene–early Eocene

Description.

Shape: subspherical, almost circular to ovoid in outline. Wall relationships: autophragm only.

Wall features: a relatively thick autophragm, with a punctate to microreticulate surface, with frequently occurring small, irregularly distributed solid, rod-like features and a maximum height of ∼ 3 µm. These features may be simple and straight to distally T-shaped.

Processes: absent.

Paratabulation: indicated by archeopyle only.

Archeopyle: relatively large, precingular, type P (3″ only); operculum free.

Paracingulum: indeterminable.

Parasulcus: indeterminable.

Dimensions. Range: overall diameter 38(45)54 µm (n = 5).

Holotype. 42 µm.

Paratypes. 45 µm.

Stratigraphic range/occurrence. Upper Paleocene–lower Eocene.

Remarks. The original description of *Pyxidinopsis* does not include any kind of projections, spines, or other possible features on the periphragm (Habib, 1975). Stover and Evitt (1978) noted that the type species, and others in the genus, most often have (micro)reticulated surfaces. Furthermore, several taxa subsequently attributed to *Pyxidinopsis*, even the type species, *P. fairhavenensis* (cf. De Verteuil and Norris, 1996), have additional wall features like coni or small projections, but none of them are like those displayed by *P. iakovlevae*. These features would not support assignment to *Operculodinium*, since the rod-like extensions are too few and of very low relief compared to the typically longer spines in taxa of the latter. Attribution to *Xenicodinium* (Klement, 1960) is refuted, since that genus is even less well defined than *Pyxidinopsis* (e.g., with an uncertain archeopyle).

Suborder Goniodomineae (Fensome et al., 1993)

Family Goniodomaceae (Lindemann, 1928)

Subfamily Goniodomoideae (autonym)

Genus *Heteraulacacysta* (Drugg and Loeblich, 1967; emend. Bujak in Bujak et al., 1980)

Heteraulacacysta pramparoae sp. nov.
Plates 3, 4, S18, S19

Derivation of name. Named for Mercedes Beatriz Pramparo, in recognition of her achievements in marine palynology, at IANIGLA, CCT-CONICET, Mendoza, Argentina.

Diagnosis. A species of *Heteraulacacysta* characterized by very thin wall layers, with isolated small rods or pillars, or rows of small "pillars", supporting the periphragm, notably around the paracingulum. Archeopyle epicystal, Type tAtP. The periphragm often appears wrinkled, but on some specimens this may faintly indicate paratabulation, overall supporting assignment to the Goniodomidae.

Holotype. Plate 3, A–H

Paratypes. Plate 4, A–C, E–H

Material. IODP 302 Hole M0004A, Lomonosov Ridge, Arctic Ocean

Type locality and horizon. IODP 302 Hole M0004A, Lomonosov Ridge, Arctic Ocean, lower Eocene sample 302-4A-27X-3-90/92 cm

Age. Early Eocene

Description.

Shape: (sub)spherical; outline circular to oval in apical/antapical view; combination epicystal archeopyle, Type tAtP.

Wall relationships: two wall layers are apparent; a thin endophragm and a periphragm are closely appressed over large parts of the cysts ("autophragm", as per Bujak in Bujak et al., 1980). The periphragm is occasionally supported by isolated small rod-like features, or small "pillars", or even rows of these, most notably around the paracingulum.

Wall features: both wall layers appear completely smooth to psilate, to incidentally microgranulate under light microscopy, except for the rod-like or pillar-like features of low relief that may occur in rows connecting the two wall layers, most notably around the paracingulum.

Processes: absent.

Paratabulation: indicated by the tAtP archeopyle, sometimes by conspicuous folds of the periphragm, and potentially in combination with the rows of small "pillars", which may also reflect sutural growth bands.

Archeopyle: formed by the release of all the apical and precingular paraplates (tAtP, compound).

Paracingulum: clearly featured by septa formed by the periphragm, supported by rows of small pillars connecting to the endophragm.

Parasulcus: indicated by a small incursion in the paracingular septae only.

Dimensions. Length/width 58 × 85 µm (n = 10).

Holotype. 61 × 77 µm.

Paratypes. 62 × 75 µm.

Stratigraphic range/occurrence. Early Eocene

Remarks. Wall morphologies, ultrastructure, and wall relationships in *Heteraulacacysta* and in the very similar genus

Dinopterygium (Deflandre, 1935). Stover and Evitt (1978) are still unclear on most species of this group of Goniodomidae. SEM/TEM analyses will be required to fully resolve such issues. The "pillars", and notably the rows of them, including the connections supporting the paracingular rim, separate *H. pramparoae* from all other described *Heteraulacacysta* species.

Suborder Gonyaulacineae

Family Gonyaulacaceae

Subfamily Gonyaulacoideae

Genus *Chaenosphaerula* (Damassa, 1997)

Chaenosphaerula sliwinskae sp. nov.
Plate 2, S15, S16

Derivation of name. Named for Kasia K. Sliwinska in recognition of her achievements in marine palynology and organic geochemistry at the Geological Survey of Denmark and Greenland (GEUS), Copenhagen, Denmark.

Diagnosis. Gonyaulacoid cysts that are solely comprised of a periphragmal parasutural network; a central body (or endophragm) is not present. These match the criteria for attribution to *Evittosphaerula* (Manum, 1979) or *Chaenosphaerula* (Damassa, 1997). The network in this case is characterized by relatively broad, irregularly shaped bands, much like the Italian pasta, *tagliatelle*, typical for *Chaenosphaerula*. Occasionally, fragments of intratabular areas, attached to the parasutural "ribbons", may be present as well. Reflected paratabulation appears gonyaulacean, matching that surmised for *Chaenosphaerula*. Archeopyle is uncertain due to the absence of all plates but most likely involves 3".

Holotype. Plate 2, A–C

Paratypes. Plate 2, D–F, G–H

Material. IODP 302 Hole M0004A, Lomonosov Ridge, Arctic Ocean

Type locality and horizon. IODP 302 Hole M0004A, Lomonosov Ridge, Arctic Ocean, lower Eocene, Core 302-0004A-27X-2-0/1

Age. Early Eocene

Description.

Shape: subspherical.

Wall relationships: solely comprise a parasutural network; central body is not present.

Wall features: parasutural network comprising relatively broad bands, reminiscent of the pasta type, *tagliatelle*, delineating a standard gonyaulacoid tabulation. Parts of intratabular areas may be represented by smooth and thin wall material.

Processes: absent.

Paratabulation: indicated by parasutural network representing the periphragm, delineating a standard gonyaulacoid tabulation.

Archeopyle: unclear because only parasutural strands are represented, but, given the presence of all parasutures, the archeopyle may be a single-plate, presumably precingular, Type P (3" only).

Paracingulum: indicated by parasutural strands.

Parasulcus: indicated by parasutural strands.

Dimensions. Diameter 65(73)85 µm ($n = 5$).

Holotype. 80 µm.

Paratypes. 75 µm, 65 µm.

Stratigraphic range/occurrence. Early Eocene

Remarks. The species is distinct from *Chaenosphaerula magnifica* by its much broader and more irregularly shaped parasutural strands.

Guersteinia gen. nov.

Type species.

Guersteinia delicata comb. nov. Williams and Downie (1966), p. 235, Pl. 26, Fig. 8

Basionyms.

Thalassiphora delicata (Williams and Downie, 1966)

Disphaeria delicata (Norvick, 1973)

Thalassiphora delicata (Eaton, 1976)

Thalassiphora delicata (Lentin and Williams, 1977)

Thalassiphora delicata (Bujak in Bujak et al., 1980)

Derivation of name. Named for G. Raquel Guerstein in recognition of her achievements in marine palynology, at the Instituto Geológico del Sur (INGEOSUR), Departamento de Geología, Bahia Blanca, Argentina.

Diagnosis. Guersteinia accommodates intermediate to large, thin-walled, camocavate, non-cribroperidinioid sexiform gonyaulacoid cysts. The small endocyst is subspherical to ellipsoidal, and the dorso-ventrally compressed, often partially tabulated periphragm is connected to the endocyst dorsally but strongly separated ventrally. It forms an umbrella-like structure. Archeopyle is precingular, formed by the detachment of paraplate 3". Operculum free.

Description.

Shape: central body (endophragm) and periphragm appear subspherical from a dorsal and ventral view, which is how it is typically oriented in slides for light microscopy.

Wall relationships: cysts camocavate. Endophragm and periphragm are appressed in the mid-dorsal area but strongly separated ventrally so that the dorso-ventrally compressed periphragm forms an umbrella-like structure.

Wall features: endophragm typically thin and smooth, occasionally scabrate. Parasutural features (e.g., traces or low ridges) are often present on the periphragm. Major paraplate boundaries appear to be at least partially reflected, indicating a standard symmetric gonyaulacoid pattern, i.e., not cribroperidinioid displaying dextral torsion.

Processes: absent.

Paratabulation: often at least partially indicated by parasutural septa and/or low ridges on the periphragm, delineating a standard symmetric sexiform gonyaulacoid tabulation.
Archeopyle: type P (3" only), detached.
Paracingulum: often indicated by parasutural features on the periphragm.
Parasulcus: typically indicated by parasutural ridges on the periphragm.
Size: intermediate to very large.
Re-attributed species.
Guersteinia delicata gen et comb. nov. Plate S17, S41
Guersteinia lacunata (Vieira et al., 2018) comb. nov.
Guersteinia succincta (Morgenroth, 1966) comb. nov.

Remarks. In a recent paper, Mudie et al. (2020) discussed wall relationships within species of *Thalassiphora* at length while describing *T. subreticulata* and *T. balcaniensis*. They provide a detailed overview of all "accepted" species included in the index of Fensome et al. (2019), noting differences in wall structure, size range, type location, and age (see their Table 2, p. 260). Importantly, in that study, the authors follow Fensome et al. (1993), who regard *Thalassiphora* as a part of the subfamily Cribroperidinioideae of the family Gonyaulacaceae. This subfamily is mainly characterized by having an "offset" hypocyst, reflecting "dextral torsion" relative to the "symmetric" sexiform gonyaulacoids. However, Mudie et al. (2020, p. 257) also note that, on some specimens, where visible, *T. balcaniensis* may be in fact be characterized as reflecting standard gonyaulacean organization rather than being cribroperidinioid. Moreover, they note that, within typical *Thalassiphora*, i.e., as in the type species *T. pelagica* and allies, the wall structures are typically thick, fibrous, and without clear reflection of paratabulation. In addition, these taxa often also show an antapical protrusion of some kind.

In the ACEX material, specimens assignable to *T. delicata* are numerous. While we can mention large variability in overall size, all these specimens may be characterized by having a distinctly thin endophragm and periphragm, with the latter showing clear paratabulation (Plate S17 and SEM image Plate S41, g). The reflected pattern is somewhat difficult to interpret because of the massive "inflation" of the periphragm. However, the typical sexiform organization of the sulcal plates and 1"" may often be discerned, and, from there, it follows that epicystal major plate sutures are reflected as well. Importantly, this taxon does not display the dextral torsion of the hypocyst relative to the epicyst that is characteristic of the cribroperidinioid lineage but rather a standard gonyaulacoid. Furthermore, its (thin) wall, the absence of an antapical protrusion, and the well-reflected paratabulation set it apart from *Thalassiphora* and its type species *T. pelagica* (Eisenack and Gocht, 1960) and from the many morphologically related genera such as *Muratodinium*, *Cordosphaeridium*, *Ifecysta*, and *Damassadinium*. Hence, based on the standard sexiform gonyaulacoid paratabulation reflected on the periphragm of the many recorded specimens of *T. delicata* and on the holotype (Williams and Downie, 1966, p. 235, Pl. 26, Fig. 8, refigured in Bujak et al., 1980, Pl. 8, Fig. 10) and its typical transparent, thin walls, we conclude that these aspects do not match the definition of the genus *Thalassiphora*. We therefore erect *Guersteinia* to accommodate this widely recorded taxon.

Recently, Vieira et al. (2018) described *Thalassiphora lacunata* from the Paleocene of NW Europe, a taxon they already considered to be morphologically closely related to *delicata*. Indeed, we concur, and we attribute that species here to *Guersteinia*.

Differential diagnosis. Guersteinia differs from *Thalassiphora* in its standard sexiform plate organization rather than the dextral torsion as recorded in all taxa within the cribroperidinioid lineage. The periphragm of *Guersteinia* is typically larger than its endocyst and is dorso-ventrally compressed, which sets it apart from *Lophocysta* (Manum, 1979). It differs from *Invertocysta* (Edwards, 1984) by the dorsally appressed endophragm and periphragm, rather than vice versa.

There are more thin-walled cavate gonyaulacoid taxa currently assigned to *Thalassiphora*, like *T. rota* (Schiøler, 2005), that clearly lack the typical overall features manifest for the former genus. Other superficially similar cavate gonyaulacoid taxa have been placed in other genera (either formally or in "open nomenclature"), e.g., *Invertocysta*, *Gelatia*, *Saturnodinium*, *Dalella*, and *Lophocysta* and perhaps even *Aiora* and likely others. For these, further studies should confirm a more precise allocation.

Sangiorgia gen. nov.

Type species. Sangiorgia pospelovae gen. et sp. nov. (Plates 9, 10, S30, S31, S32, 33)

Derivation of name. Named for Francesca Sangiorgi in recognition of her achievements in marine palynology, at the Laboratory of Palaeobotany and Palynology, Department of Earth Sciences, Utrecht University, the Netherlands.

Diagnosis. Cysts proximochorate to skolochorate; intermediate to large in size, body subspherical, bearing isolated gonal, relatively large, solid processes, of which many, but typically not all, distally interconnect. Such processes are distally interconnected with ribbon-like features, sometimes evolved into "tramlines" typical for *Nematosphaeropsis* and sometime single connections such as in *Cannosphaeropsis*, and these connections may be locally clustered on larger portions of the cyst. Distally, the essentially "gonal" locations may be marked by trifurcate projections. Proximal markings between process bases absent or limited to faint parasutural lines; paratabulation standard sexiform gonyaulacacean; archeopyle precingular, Type P, operculum free.

Description.
Shape: body subspherical.
Wall relationships: autophragm only, or endophragm and periphragm appressed between processes.

Wall features: autophragm smooth or faintly ornamented. Parasutural features between process bases faint (e.g., traces of low ridges) or absent altogether; features may be present over entire cyst or only locally.

Processes: gonal only or gonal and intergonal; tips of unconnected processes may distally be trifurcate (gonal) or bifurcate (intergonal). A variable portion of the processes distally link to form trabeculae that connect several processes, sometimes leading to a partial and incomplete parasutural network. Connections between processes may comprise one (as in *Cannosphaeropsis*) or two (as in *Nematosphaeropsis*) trabeculae.

Paratabulation: gonal processes and faint sutural ornamentation indicate standard sexiform gonyaulacacean tabulation.

Archeopyle: precingular, Type P (3" only); operculum free.

Paracingulum: indicated, if at all, by parasutural lines and position of gonal processes.

Parasulcus: indicated, if at all, by parasutural lines.

Size: medium.

Type species.

Sangiorgia pospelovae sp. nov. (this paper)

Other species.

Sangiorgia marretiae sp. nov. (this paper)

Remarks. Sangiorgia is a genus with the basic building plan of *Spiniferites* and allied genera. Systematically, it resembles *Achomosphaera* because of the sparse parasutural ornamentation but differs in having distal connections of only a portion of the gonal processes. In *Nematosphaeropsis* and *Cannosphaeropsis*, all processes are distally connected (simple, or by "tramlines") to form a complete network around the central body, whereas only part of the processes are interconnected in *Sangiorgia*.

Sangiorgia pospelovae gen. et sp. nov.
Plates 9, 10, S30, S31, S32, 33

Derivation of name. Named for Vera Pospelova in recognition of her achievements in marine palynology, at the Department of Earth and Environmental Sciences, University of Minnesota, Minneapolis, USA.

Diagnosis. Cysts skolochorate; intermediate to large; body subspherical; bearing isolated essentially gonal; relatively large, solid, processes, of which many, but typically not all, distally interconnect. The distal connections are formed by ribbon-like features, typical for *Cannosphaeropsis*, sometimes evolved into "tramlines" typical for *Nematosphaeropsis*. The distally interconnected processes typically form clusters, giving the cysts an irregular outline. Proximal markings between process bases are absent or limited to faint parasutural lines; paratabulation standard sexiform gonyaulacacean; archeopyle precingular, Type P, operculum free.

Holotype. Plate 9, A–D

Paratypes. Plate 9, E–H, I–L; Plate 10, E–H

Material. IODP 302 Hole M0004A, Lomonosov Ridge, Arctic Ocean

Type locality and horizon. IODP 302 Hole M0004A, Lomonosov Ridge, Arctic Ocean, lower Eocene, cores 302-0004A-28X-2-130/132

Age. Early Eocene

Description.

Shape: central body subspherical, outline skolochorate, but irregular in consequence of sets of groups of clustered, distally partially connected processes, combined with occasional single, distally not connected gonal processes.

Wall relationships: autophragm only, or endophragm and periphragm "appressed" between processes.

Wall features: autophragm smooth or faintly ornamented. Parasutural features between process bases faint (e.g., traces of low ridges) or absent altogether; features may be present over entire cyst or only locally.

Processes: gonal only, or gonal and intergonal; tips of unconnected processes may distally be broadly trifurcate (gonal) or bifurcate (intergonal). A variable portion ("sets") of processes distally link to form rather thick trabeculae that connect several processes, sometimes leading to a partial and incomplete distal parasutural network. Connections between (sets of) processes may comprise one (as in *Cannosphaeropsis*) or two (as in *Nematosphaeropsis*) trabeculae.

Paratabulation: positions of gonal processes and faint sutural ornamentation indicate standard sexiform gonyaulacacean tabulation.

Archeopyle: precingular, Type P (3" only); operculum free.

Paracingulum: indicated, if at all, by parasutural lines and position of gonal processes.

Parasulcus: indicated, if at all, by parasutural lines.

Dimensions. central body 35(40)42 (L) ×30(38)40 (W) ($n = 10$); total dimensions 60(70)77 (L) ×63(68)75 (W)

Holotype. Central body/total: 40/70 µm (L) ×38/68 µm (W).

Paratypes. Central body/total: 35/77 (L) ×30/63 (W) µm, central body/total: 40/70 (L) µm ×40/70 (W) µm, central body/total: 42/68 (L) µm ×36/70 (W) µm

Stratigraphic range/occurrence. Early Eocene

Remarks. Sangiorgia pospelovae somewhat resembles *Achomosphaera alcicornu* in overall character but has distinctly distally connected (sets of) processes. It differs from *S. marretiae* in being more robust and larger, having rather thick trabeculae, but foremost in the distinct lack of tri- or bifurcated processes positioned distally on top of the connecting trabeculae, "barbed wire style".

Sangiorgia marretiae sp. nov.
Plates 8, S28, S29

Etymology. Named for Fabienne Marret-Davies in recognition of her achievements in marine palynology, at Liverpool University, United Kingdom.

Diagnosis. Cysts proximochorate; small to intermediate in size, body subspherical, bearing gonal and intergonal, solid processes, of which many, but not all, distally interconnect. The connections are formed by single, ribbon-like trabecular features, which sometimes split into two strands, like the "tramlines" typical for *Nematosphaeropsis*. The gonal locations are typically distally marked by somewhat broad, trifurcate projections, typical for *Spiniferites* species. However, since these tri- and occasionally bifurcations occur distally on top of the connecting trabeculae, the overall habitus is also reminiscent of species of *Cannosphaeropsis*, notably *C. utinensis*(e.g., "barbed wire style" distal trabeculae). Proximal markings between process bases are limited to faint parasutural lines; paratabulation standard sexiform gonyaulacacean, like all members of the spiniferitioids; archeopyle precingular, Type P, operculum free.

Holotype. Plate 8, E–H

Paratypes. Plate 8, A–D, I–L

Material. IODP 302 Hole M0004A, Lomonosov Ridge, Arctic Ocean

Type locality and horizon. IODP 302 Hole M0004A, Lomonosov Ridge, Arctic Ocean, lower Eocene, Core 302-0004A-27X-3-80/82

Age. Early Eocene

Description.

Shape: body subspherical.

Wall relationships: autophragm only, or endophragm and periphragm "appressed" between processes.

Wall features: autophragm smooth or faintly ornamented. Parasutural features between process bases faint (e.g., traces of low ridges) or absent altogether; features may be present over entire cyst or locally.

Processes: gonal only, or gonal and intergonal; tips of connected and unconnected processes are distally trifurcate (gonal) or bifurcate (intergonal) and occur on top of the distally connecting trabeculae. A variable portion of the processes distally links to form trabeculae that connect several processes, sometimes leading to a partial and incomplete parasutural network. Connections between processes may comprise one (as in *Cannosphaeropsis*) or two (as in *Nematosphaeropsis*) trabeculae.

Paratabulation: positions of gonal processes and faint sutural ornamentation indicates standard sexiform gonyaulacacean (Spiniferitioid) tabulation.

Archeopyle: precingular, Type P (3" only); operculum free.

Paracingulum: indicated, if at all, by parasutural lines and position of gonal processes.

Parasulcus: indicated, if at all, by parasutural lines.

Dimensions. Diameter central body 22(28)35 µm ($n = 10$).

Holotype. 28 µm.

Paratypes. 35 µm, 22 µm.

Stratigraphic range/occurrence. Early Eocene

Remarks. It differs from *S. pospelovae* in being thin-walled, more fragile, transparent, and smaller and by the presence of distal, tri- or bifurcated processes occurring on top of the distally connecting trabeculae. In overall habitus and variations, this species superficially comes across as a *Spiniferites* but differs by forming a distinct, but incomplete, distally connecting network of essentially simple (sets of) strands or trabeculae.

Subfamily Leptodinioideae

Genus *Spiniferella* (Stover and Hardenbol, 1994)

Spiniferella crouchiae sp. nov.
Plates 7, S24

Etymology. Named for Erica Crouch in recognition of her achievements in marine palynology, at GNS Science, Lower Hutt, New Zealand.

Diagnosis. A species of *Spiniferella* characterized by its large size, with long gonal processes, which terminate in trifurcate ends, that may individually split again into secondary bifurcations or even trifurcations. Proximal markings between process bases are limited to faint parasutural lines; paratabulation standard sexiform gonyaulacacean, like all members of the spiniferitioids; archeopyle precingular, Type P, operculum free.

Holotype. Plate 7, A–B

Paratypes. Plate 7, C and D

Material. IODP 302 Hole M0004A, Lomonosov Ridge, Arctic Ocean

Type locality and horizon. IODP 302 Hole M0004A, Lomonosov Ridge, Arctic Ocean, lower Eocene, Core 302-0004A-27X-3-50/52

Age. Early Eocene

Description.

Shape: body subspherical.

Wall relationships: autophragm only or endophragm and periphragm appressed between processes.

Wall features: autophragm smooth to granulate to reticulate. Prominent parasutural ridges between process bases, like those in the type species *Spiniferella cornuta* (Stover and Hardenbol, 1994).

Processes: gonal only; tips trifurcate, with often secondary bi- and trifurcations.

Paratabulation: positions of gonal processes and faint sutural ornamentation indicate standard sexiform, L-type, gonyaulacacean tabulation.

Archeopyle: precingular, Type P (3″ only); operculum free.

Paracingulum: indicated by parasutural ridges or septa and the position of gonal processes.

Parasulcus: indicated by parasutural ridges or septa.

Dimensions. Total diameter 125(135)150 µm ($n = 10$), central body 70(75)80 µm ($n = 10$).

Holotype. Total 130 µm, central body 80 µm.
Paratypes. 140/65 µm; 130/70 µm.
Stratigraphic range/occurrence. Early Eocene
Remarks. It differs from *Spiniferella cornuta* by its extraordinary large size and by typical secondary bifurcated or trifurcated endings of the rather long trifurcated gonal spines.

6.2 Photo plates

Codes in the plate captions represent sample codes (core, section, and interval following IODP convention) and England Finder coordinates. The Supplement includes 38 light microscope photoplates and 3 SEM plates, of which high-resolution versions are available on Zenodo (Sluijs and Brinkhuis, 2024, version 4: https://doi.org/10.5281/zenodo.10998747).

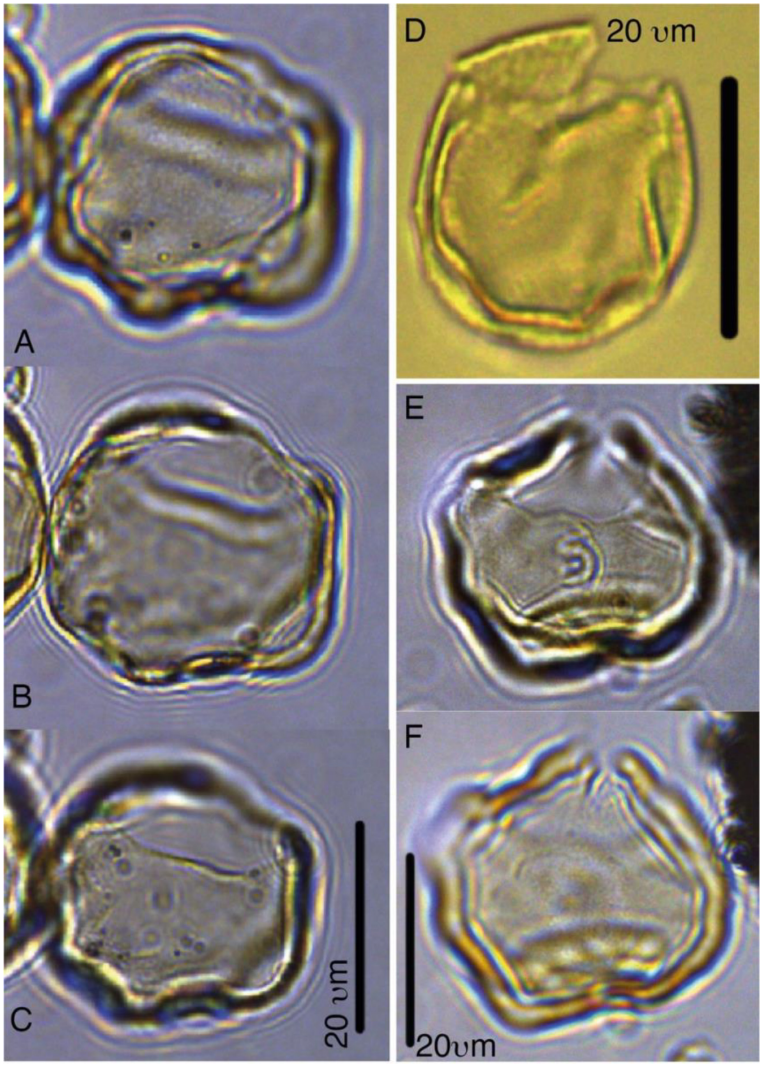

Plate 1. *Batiacasphaera obohikuenobeae.* **(a–c)** Holotype, 27X-2-03/04 cm, slide 1, R23-1. **(d)** 27-X-3-30/32 cm, slide 1, G17-4. **(e–f)** Paratype, 27X-2-03/04 cm, slide 1, P22-3.

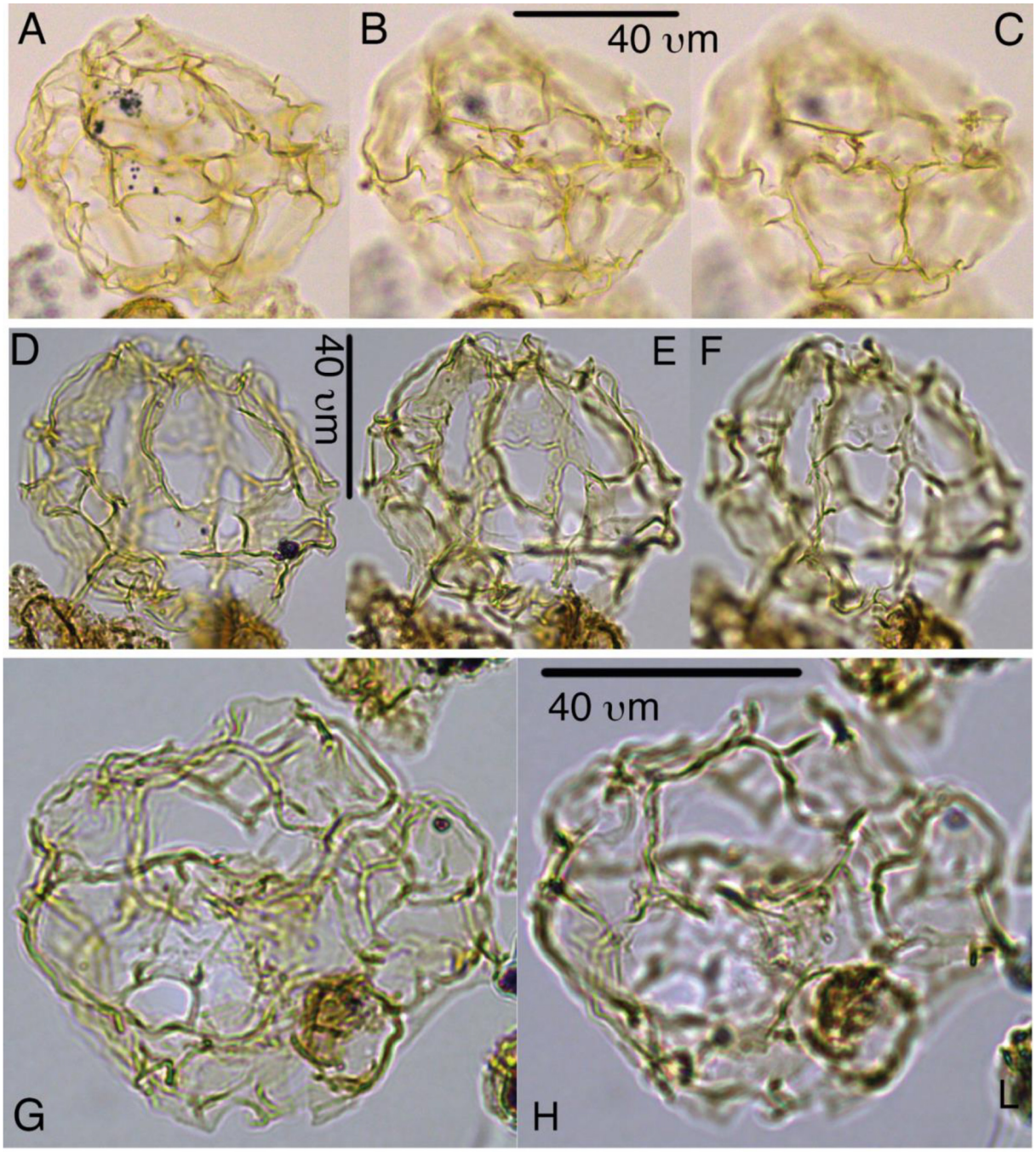

Plate 2. *Chaenosphaerula sliwinskae*. **(a–c)** Holotype, 27X-2-00/02 cm, slide 1, Q39-2. **(d–f)** Paratype, 27X-2-14/16 cm, slide 1, O33-3. **(g–h)** Paratype, 27X-2-20/21 cm, slide 1, E13-4.

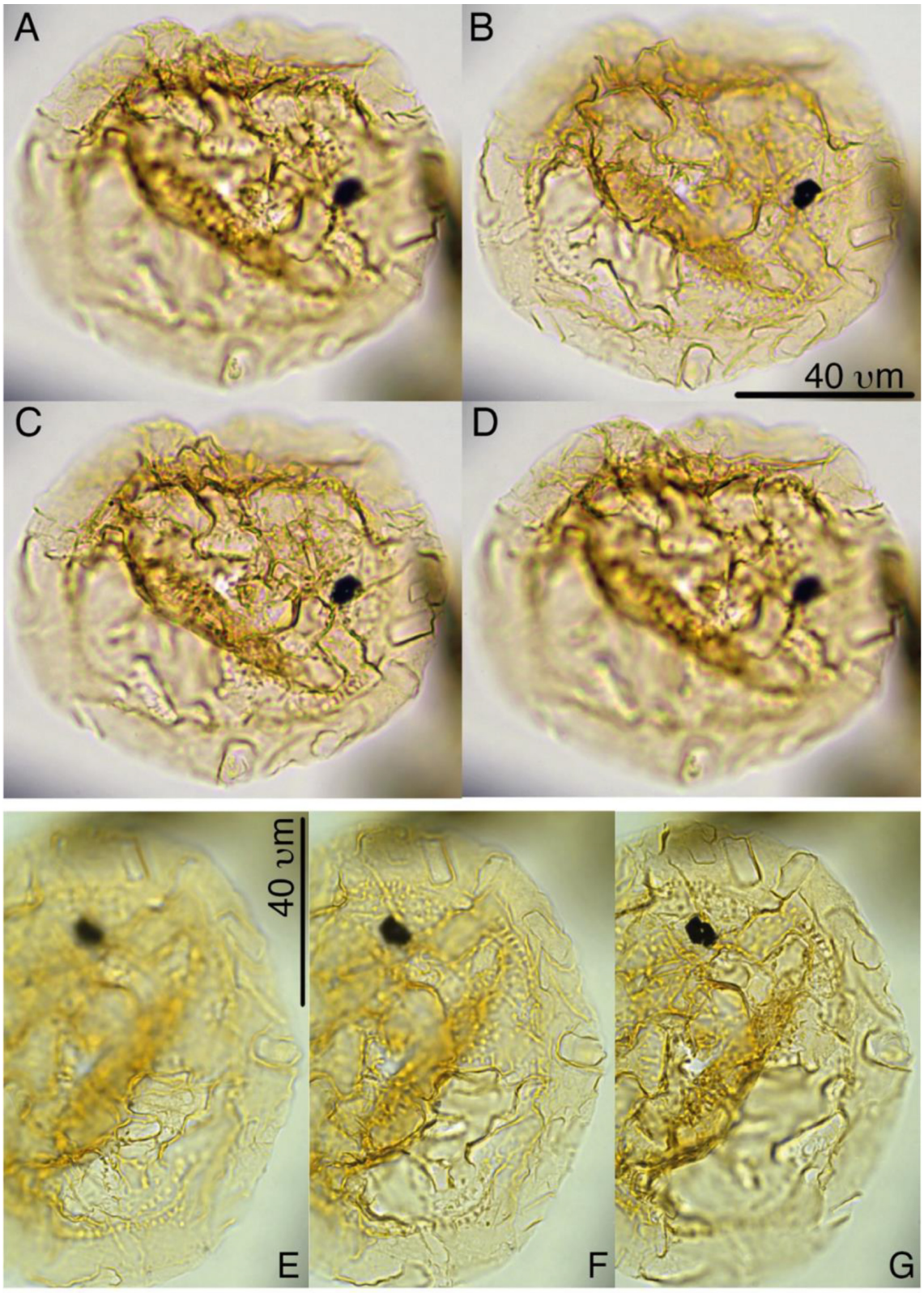

Plate 3. *Heteraulacacysta pramparoae*. **(a–g)** Holotype, 27X-3-90/92 cm, slide 1, K22.

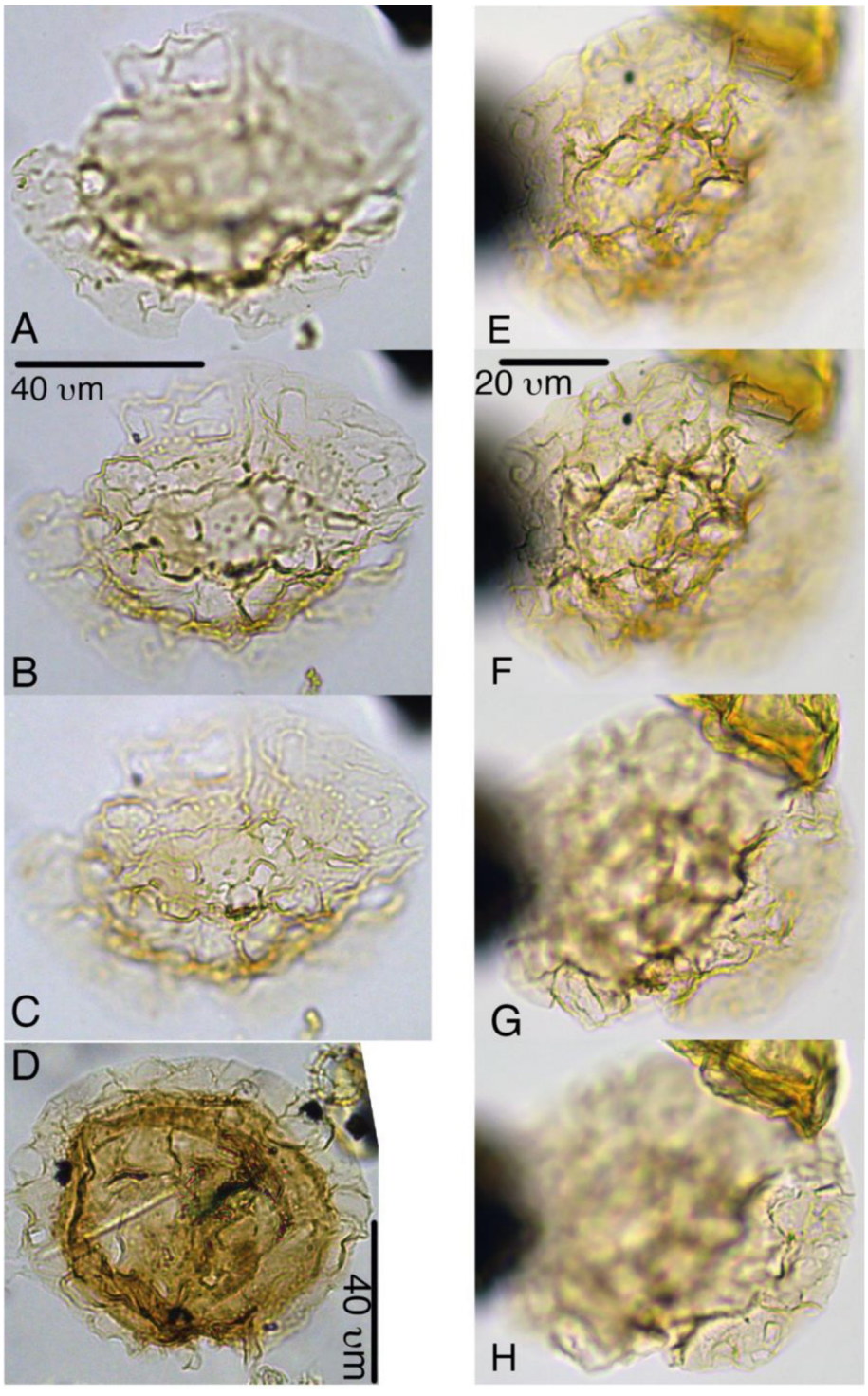

Plate 4. *Heteraulacacysta pramparoae*. **(a–c)** Paratype, 27X-3-1-110/112 cm, slide 2, H17. **(d)** 27X-2-20/21 cm, slide 1, B19-4. **(e–h)** Paratype, 27X-3-90/92 cm, slide 1, D17.

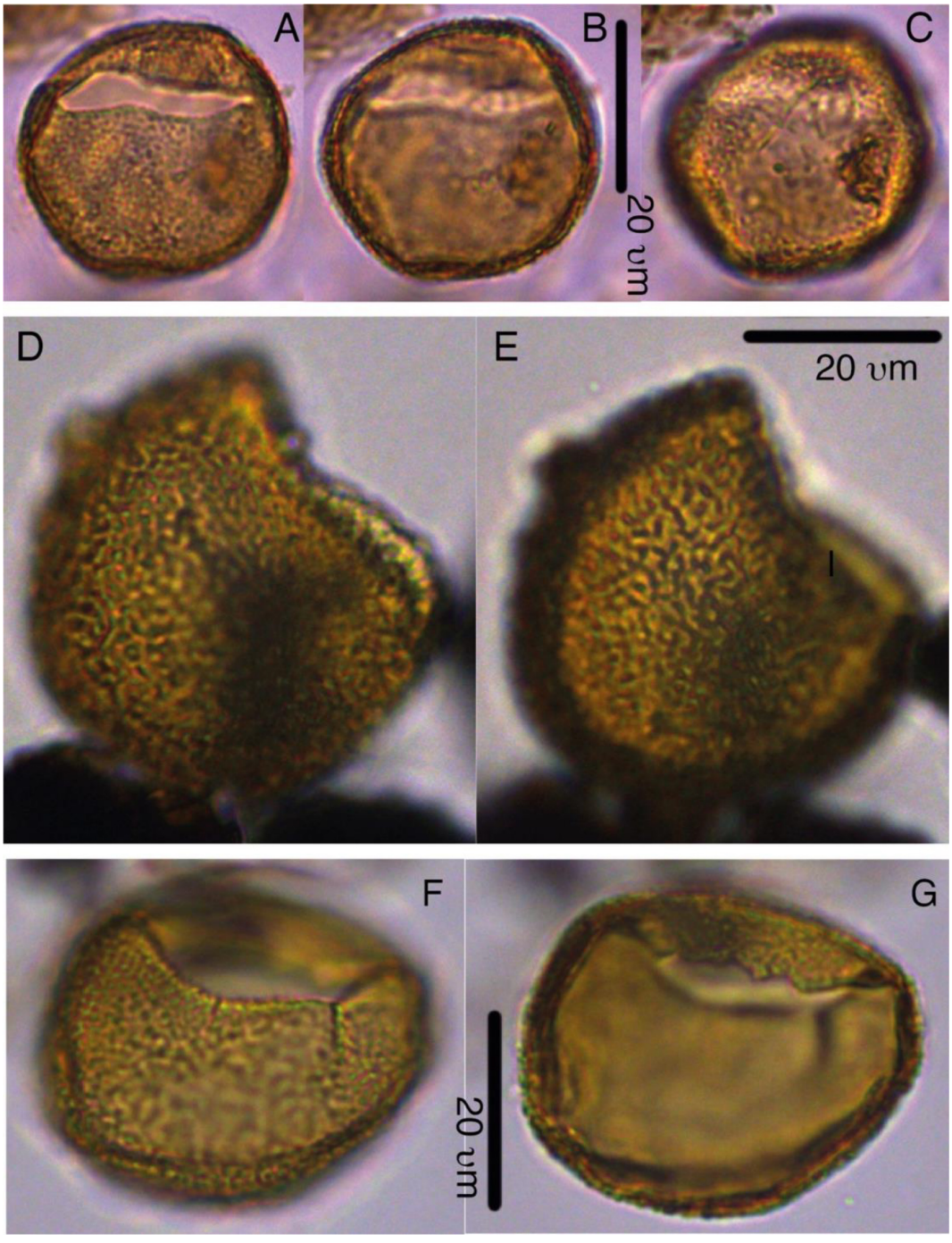

Plate 5. *Pyxidinopsis iakovlevae.* **(a–c)** Paratype, 27X-1-10/12 cm, slide 2, W30-1. **(d–e)** Paratype, 33X-CC, slide 1, K13-1. **(f–g)** Paratype, 33X-CC, slide 1, V22-4.

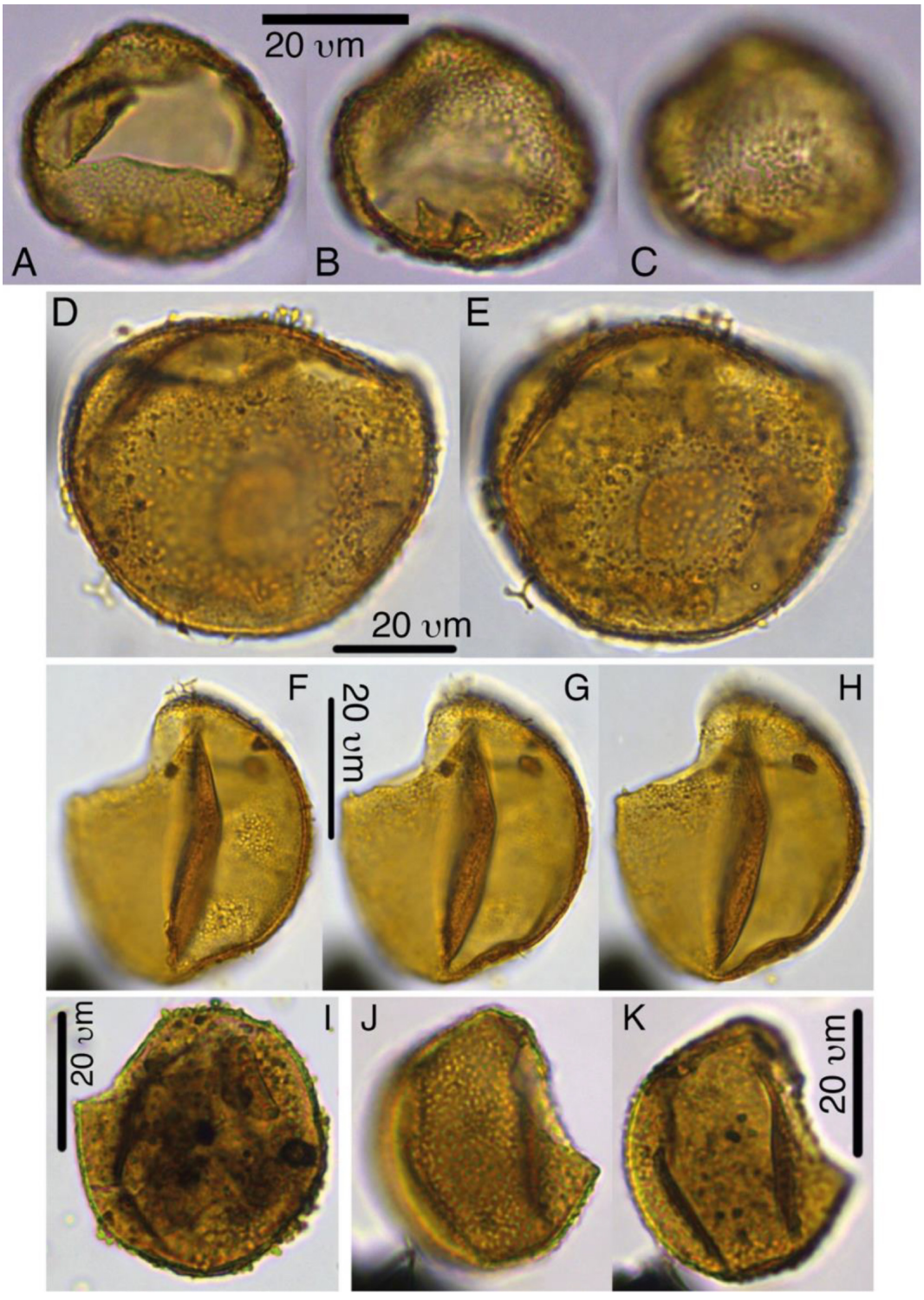

Plate 6. *Pyxidinopsis iakovlevae*. **(a–c)** Holotype, 27X-3-20/22 cm, slide 1, W14-4. **(d–e)** Paratype, 27X-1-10/12 cm, slide 2, H27-4. **(f–g)** Paratype, 27X-3-50/52 cm, slide 2, M20-1. **(i)** 32X-2-81/83 cm, slide 1, L-41. **(j–k)** 32X-CC, F29-3.

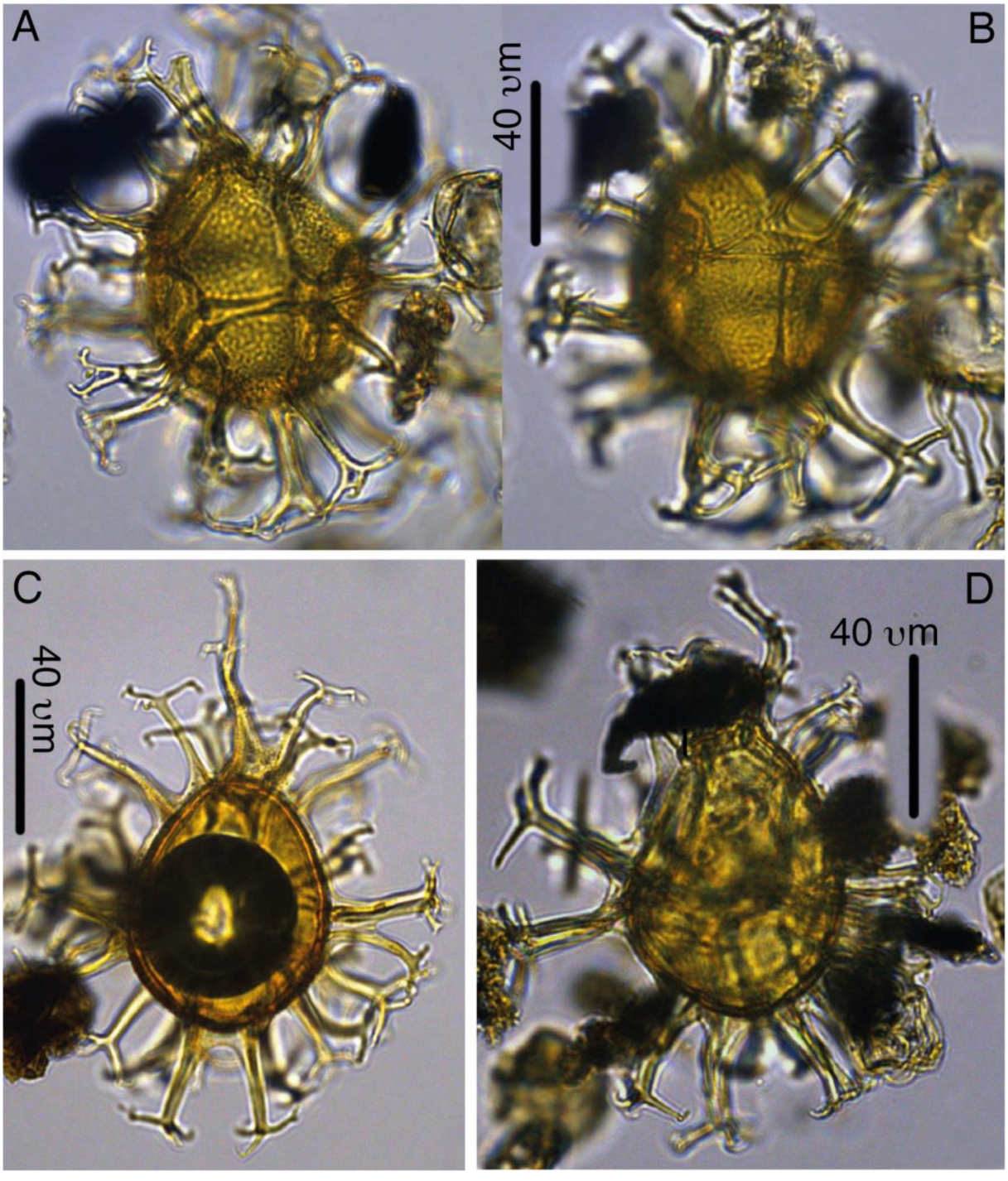

Plate 7. *Spiniferella crouchiae*. **(a–b)** Holotype, 27X-3-50/52, slide 1, N26-4. **(c)** Paratype, 27X-2-20/21 cm, slide 1, C19-1. **(d)** Paratype, 27X-3-30/32, slide 1, K27.

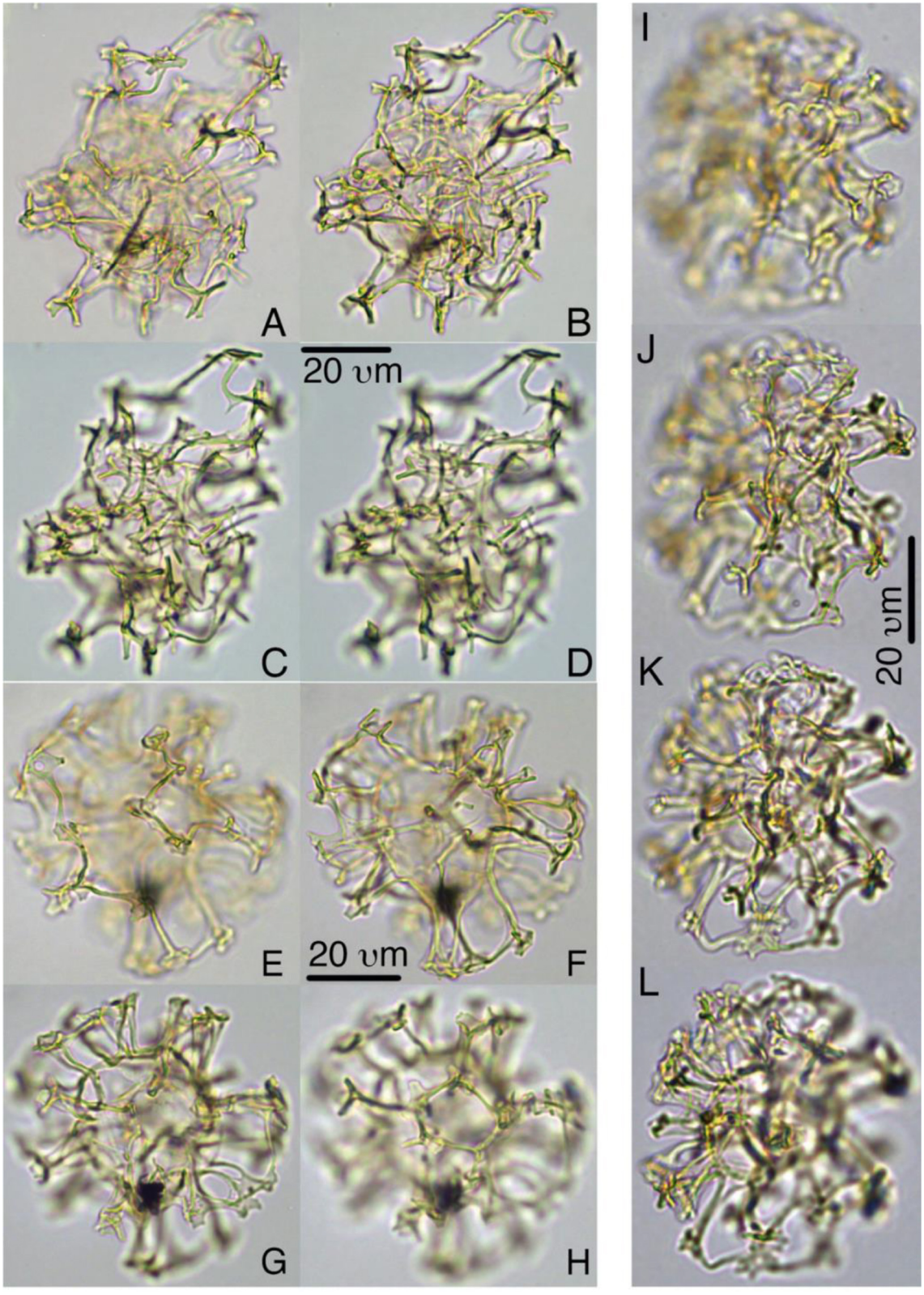

Plate 8. *Sangiorgia marretiae*. **(a–d)** Paratype, 27X-3-80/82 cm, slide 1, G27-1. **(e–h)** Holotype, 27X-3-80/82 cm, slide 1, S25-2. **(i–l)** Paratype, 27X-3-80/82 cm, slide 1, O31-1.

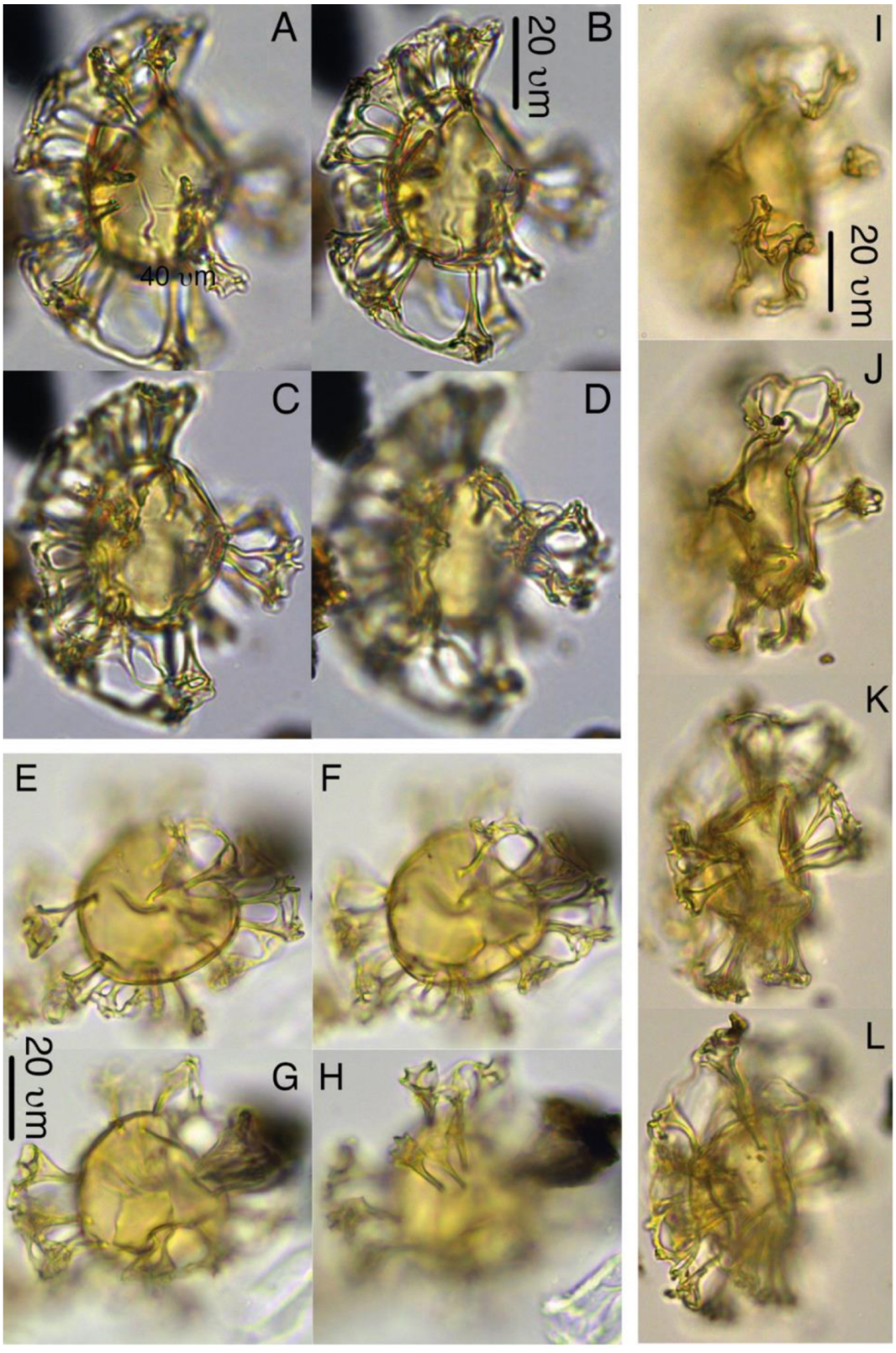

Plate 9. *Sangiorgia pospelovae*. **(a–d)** Holotype, 28X-2-130/132 cm, slide 1, J27-2. **(e–h)** Paratype, 28X-40/42, slide 1, U20-4. **(i–l)** Paratype, 27X-4-10/12 cm, slide 1, L27-4.

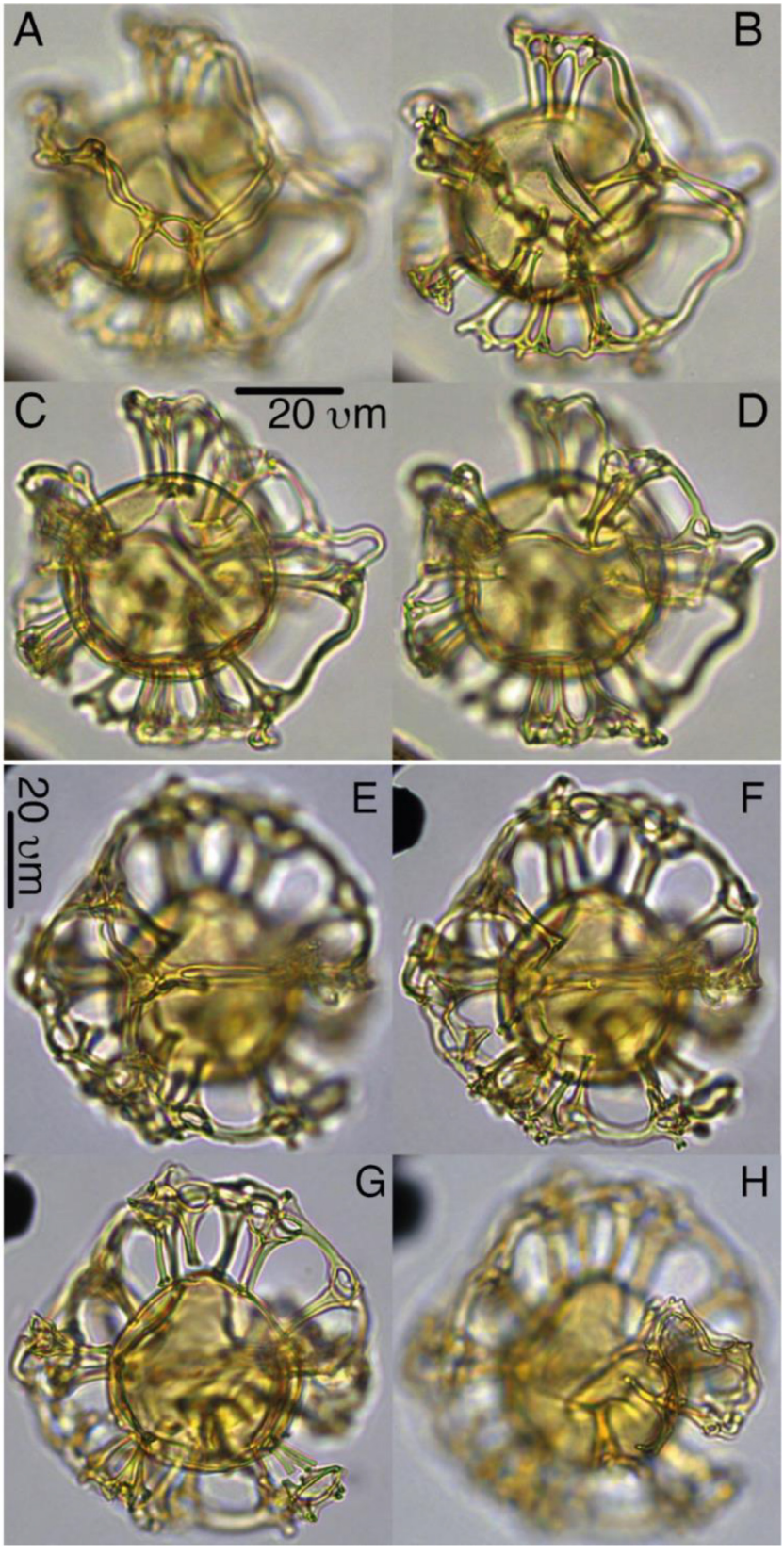

Plate 10. *Sangiorgia pospelovae.* **(a–d)** 27X-3-60/62 cm, slide 1, L25-3. **(e–h)** Paratype, 27X-3-80/82 cm, slide 1, L17-4.

6.3 Species list, taxonomic remarks, and taxonomical/ecological grouping

Listed below are all encountered species. Between brackets are the taxonomical/paleoecological groups they have been included in for our quantitative analysis.

Achomosphaera alcicornu (*Spiniferites* cpx)
Achomosphaera ramulifera (*Spiniferites* cpx)
Achomosphaera spp. (pars.) (*Spiniferites* cpx)
Adnatosphaeridium spp. (other G-cysts)
Alisocysta heilmannii (other G-cysts)
Alisocysta circumtabulata (other G-cysts)
Alisocysta margarita (other G-cysts)
Alisocysta reticulata (other G-cysts)
Apectodinium augustum. Remarks: we note that many specimens are somewhat small (*Apectodinium* spp.).
Apectodinium homomorphum (*Apectodinium* spp.; wetzelielloids)
Apectodinium hyperacanthum (*Apectodinium* spp.; wetzelielloids)
Apectodinium parvum (*Apectodinium* spp.; wetzelielloids). Remarks: some specimens of *A. parvum* could be confused with *Wilsonidium*.
Apectodinium quinquelatum. Remarks: we note that many specimens are somewhat small. (*Apectodinium* spp.; wetzelielloids)
Apectodinium summissum (*Apectodinium* spp.; wetzelielloids)
Apectodinium spp. (pars; *Apectodinium* spp.; wetzelielloids).
Apteodinium spp. (other G-cysts)
Areoligera coronata (*Areoligera* cpx)
Areoligera medusettiformis (*Areoligera* cpx)
Areoligera senonensis (*Areoligera* cpx)
Areoligera spp. (pars) (*Areoligera* cpx)
Batiacasphaera obohikuenobeae sp. nov. (other G-cysts)
Batiacasphaera spp. (pars). Remarks: this group includes only specimens with a size like *B. compta*, thus much larger than *B. obohikuenobeae* (other G-cysts)
Caligodinium aceras (other G-cysts)
Cannosphaeropsis spp. (other G-cysts)
Cerebrocysta waipawaense (other G-cysts)
Cerodinium depressum. Remarks: includes very big specimens (*Cerodinium* cpx; hexa-2A peridinioids; low-salinity-tolerant)
Cerodinium speciosum (*Cerodinium* cpx; hexa-2A peridinioids; low-salinity-tolerant)
Cerodinium striatum Remarks: includes very small specimens (*Cerodinium* cpx; hexa-2A peridinioids; low-salinity-tolerant)
Cerodinium wardenense (*Cerodinium* cpx; hexa-2A peridinioids; low-salinity-tolerant)
Cerodinium spp. (pars.) Remarks: this includes numerous strongly denticulate specimens, reminiscent of the ornamentation of *Deflandrea denticulata*. (*Cerodinium* cpx; hexa-2A peridinioids; low-salinity-tolerant)
Chaenosphaerula sliwinskae sp. nov. (other G-cysts)
Cleistosphaeridium placacanthum (other G-cysts)
Cordosphaeridium fibrospinosum (*Cordosphaeridium fibrospinosum* cpx; other G-cysts)
Cordosphaeridium fibrospinosum cpx. Remarks: this includes all specimens within this complex that could not be determined to the genus level. (*Cordosphaeridium fibrospinosum* cpx; other G-cysts)
Cribroperidinium spp.
Dapsilidinium spp. (other G-cysts)
Deflandrea denticulata Remarks: we have found numerous specimens that are difficult to distinguish from strongly denticulate forms of *Cerodinium* in this material if the shape and size of the archeopyle cannot be determined (*Cerodinium* cpx; hexa-2A peridinioids; low-salinity-tolerant)
Deflandrea oebisfeldensis (*Cerodinium* cpx; hexa-2A peridinioids; low-salinity-tolerant)
Deflandrea phosphoritica Remarks: we have encountered morphotypes with a "spongy" wall and with striations on its central body. (*Cerodinium* cpx; hexa-2A peridinioids; low-salinity-tolerant)
Deflandrea spp. (pars) (*Cerodinium* cpx; hexa-2A peridinioids; low-salinity-tolerant)
Diphyes colligerum (other G-cysts)
Dracodinium pachydermum (wetzelielloids)
Elytrocysta spp. Remarks: we have encountered morphotypes ranging from standard transparent to pale yellow to yellow. Moreover, specimens show vague to clear paratabulation reflected in the organization of the processes. Because the ectophragm is not always preserved, specimens might be confused with *Histiocysta*. (*Elytrocysta* cpx)
Eocladopyxis spp. (other G-cysts)
Fibrocysta spp. Remarks: some specimens have very slender processes. (other G-cysts)
Glaphyrocysta ordinata (*Areoligera* cpx)
Glaphyrocysta pastielsii (*Areoligera* cpx)
Glaphyrocysta spp. (pars) (*Areoligera* cpx)
Guersteinia delicata gen. et comb. nov. (other G-cysts)
Hafniasphaera septata (*Spiniferites* cpx)
Heteraulacacysta pramparoae (epicystal Goniodomidae; other G-cysts)
Homotryblium spp. (epicystal Goniodomidae; other G-cysts)
Histiocysta spp. (*Elytrocysta* cpx)
Hystrichokolpoma salacia (other G-cysts)
Hystrichokolpoma spp. (other G-cysts)
Hystrichosphaeridium tubiferum We encountered many specimens of *H. tubiferum* with a strongly axially elongated central body (see Plates S20, S21), notably in the upper part of the studied interval (Core 27X). Moreover, the shape of the processes is highly variable. We

have also encountered specimens in which the processes are distally closed by a membrane, reminiscent of *H. truswelliae* (other G-cysts).

Hystrichostrogylon spp. (*Spiniferites* cpx; other G-cysts)

Impagidinium dispertitum (other G-cysts)

Impagidinium spp. (pars.; other G-cysts)

Impletosphaeridium spp. (other G-cysts)

Kallosphaeridium brevibarbatum (other G-cysts)

Lejeunecysta spp. (Protoperidinioid; low-salinity-tolerant)

Lentinia serrata (*Cerodinium* cpx; hexa-2A peridinioids; low-salinity-tolerant)

Lentinia wetzelii (*Cerodinium* cpx; hexa-2A peridinioids; low-salinity-tolerant)

Lentinia spp. (pars). Remarks: we note large variability among *Lentinia* types, including very small, large, striate, psilate, denticulate, and transparent specimens and including intermediates. (*Cerodinium* cpx; hexa-2A peridinioids; low-salinity-tolerant)

Melitasphaeridium pseudorecurvatum (other G-cysts)

Microdinium ornatum (*Elytrocysta* cpx)

Minisphaeridium latirictum (other G-cysts)

Muratodinium fimbriatum (*Cordosphaeridium fibrospinosum* cpx; other G-cysts)

Oligosphaeridium spp. (other G-cysts)

Operculodinium spp. Remarks: we encountered several morphotypes, dominantly those encountered globally in time-equivalent strata (e.g., Plate 6 C-D of Sluijs and Brinkhuis, 2009), but also large specimens that can be confused with *Fibrocysta*, specimens with processes resembling those of *O. janduchenei*, and specimens resembling *O. microtrianium* (*Operculodinium* spp.).

Palaeocystodinium australinum (Protoperidinioid; low-salinity-tolerant)

Palaeocystodinium spp. (pars). Remarks: we encountered some very small specimens (Protoperidinioid; low-salinity-tolerant)

Phelodinium magnificum (protoperidinioid; low-salinity-tolerant)

Phelodinium spp. (pars.) (protoperidinioid; low-salinity-tolerant)

Phthanoperidinium echinatum (*Senegalinium* cpx; hexa-2A peridinioids; low-salinity-tolerant)

Phthanoperidinium spp. (pars.) (*Senegalinium* cpx; hexa-2A peridinioids; low-salinity-tolerant)

Polysphaeridium spp. This includes specimens reminiscent of *P. zoharyi*. (Epicystal Goniodomidae; other G-cysts)

Pyxidinopsis iakovlevae sp. nov. (other G-cysts)

Rottnestia borussica (*Spiniferites* cpx)

Sangiorgia pospelovae gen. et sp. nov. (*Spiniferites* cpx)

Sangiorgia marretiae gen. et sp. nov. (*Spiniferites* cpx)

Selenopemphix nephroides (protoperidinioid; low-salinity-tolerant)

Selenopemphix selenoides (protoperidinioid; low-salinity-tolerant)

Senegalinium obscurum (*Senegalinium* cpx; hexa-2A peridinioids; low-salinity-tolerant)

Senegalinium dilwynense (*Senegalinium* cpx; hexa-2A peridinioids; low-salinity-tolerant)

Senegalinium spp. (pars). Remarks: we encountered a wide variety of morphologies within *Senegalinium*, including large variations in size, degree of discernible paratabular ridges, subtle to big granulations (sometimes resembling *Vozzhennikovia*), various types of cavation (notably cornucavate at the apical horn), and specimens with a brown endophragm or entirely brown specimens, resembling *Lentinia* if the archeopyle could not be discerned. (*Senegalinium* cpx; hexa-2A peridinioids; low-salinity-tolerant)

Spinidinium densispinatum (*Senegalinium* cpx; hexa-2A peridinioids; low-salinity-tolerant)

Spinidinium spp. (pars) (*Senegalinium* cpx; hexa-2A peridinioids; low-salinity-tolerant)

Spiniferella cornuta magna spp. nov. (*Spiniferites* cpx).

Spiniferites ramosus (*Spiniferites* cpx)

Spiniferites pseudofurcatus (*Spiniferites* cpx)

Spiniferites spp. (pars). Remarks: this also includes sometimes very large specimens that show reduced penitabular ridges (towards *Achomosphaera*). (*Spiniferites* cpx)

Tectatodinium spp. (other G-cysts)

Thalassiphora pelagica (*Cordosphaeridium fibrospinosum* cpx; other G-cysts)

Wetzeliella articulata (wetzelielloids)

Wetzeliella meckelfeldensis (wetzelielloids)

Data availability. All raw data are included in a permanent online repository (Sluijs and Brinkhuis, 2024) (https://doi.org/10.5281/zenodo.10998747, version 4). A high-resolution version of the Supplement photoplates (38 plates with light microscope photos and 3 plates with scanning electron microscope photos) is also available under the same Zenodo record.

Supplement. The supplement related to this article is available online at: https://doi.org/10.5194/jm-43-441-2024-supplement.

Author contributions. AS and HB did all the work and are frankly a bit sad that they finished it.

Competing interests. The contact author has declared that neither of the authors has any competing interests.

Disclaimer. Publisher's note: Copernicus Publications remains neutral with regard to jurisdictional claims made in the text, published maps, institutional affiliations, or any other geographical representation in this paper. While Copernicus Publications makes ev-

ery effort to include appropriate place names, the final responsibility lies with the authors.

Acknowledgements. We thank the International Ocean Discovery Program and predecessors for samples and data and the science party of the Arctic Coring Expedition (2004) for their scientific and collaborative efforts. We thank Natasja Welters and Giovanni Dammers (Geolab, Utrecht University) for palynological processing and Gea Zijlstra (Utrecht University) for advice regarding the nomenclature of the newly described taxa. We also thank Ian Harding and an anonymous reviewer for their constructive and detailed analysis of the originally submitted version of this work.

Financial support. This project was funded by a European Research Council Consolidator Grant (grant no. 771497), awarded to Appy Sluijs under the Horizon 2020 program.

Review statement. This paper was edited by Luke Mander and reviewed by Ian Harding and one anonymous referee.

References

Backman, J., Moran, K., McInroy, D. B., Mayer, L. A., and the Expedition 302 Scientists: Proceedings of the Integrated Ocean Drilling Program, 302, Integrated Ocean Drilling Program Management International, Inc., Edinburgh, https://doi.org/10.2204/iodp.proc.302.2006, 2006.

Backman, J., Jakobsson, M., Frank, M., Sangiorgi, F., Brinkhuis, H., Stickley, C., O'Regan, M., Løvlie, R., Pälike, H., Spofforth, D., Gattacecca, J., Moran, K., King, J., and Heil, C.: Age model and core-seismic integration for the Cenozoic Arctic Coring Expedition sediments from the Lomonosov Ridge, Paleoceanography, 23, PA1S03, https://doi.org/10.1029/2007PA001476, 2008.

Barke, J., Abels, H. A., Sangiorgi, F., Greenwood, D. R., Sweet, A. R., Donders, T., Reichart, G.-J., Lotter, A. F., and Brinkhuis, H.: Orbitally forced Azolla blooms and Middle Eocene Arctic hydrology: Clues from palynology, Geology, 39, 427–430, https://doi.org/10.1130/G31640.1, 2011.

Bijl, P. K., Brinkhuis, H., Egger, L. M., Eldrett, J. S., Frieling, J., Grothe, A., Houben, A. J. P., Pross, J., Śliwińska, K. K., and Sluijs, A.: Comment on '*Wetzeliella* and its allies – the "hole" story: a taxonomic revision of the Paleogene dinoflagellate subfamily Wetzelielloideae' by Williams et al. (2015), Palynology, 41, 423–429, https://doi.org/10.1080/01916122.2016.1235056, 2016.

Bijl, P. K., Frieling, J., Cramwinckel, M. J., Boschman, C., Sluijs, A., and Peterse, F.: Maastrichtian–Rupelian paleoclimates in the southwest Pacific – a critical re-evaluation of biomarker paleothermometry and dinoflagellate cyst paleoecology at Ocean Drilling Program Site 1172, Clim. Past, 17, 2393–2425, https://doi.org/10.5194/cp-17-2393-2021, 2021a.

Bijl, P. K., Guerstein, G. R., Jaimes, E. A. S., Sluijs, A., Casadio, S., Valencia, V., Amenábar, C. R., and Encinas, A.: Campanian-Eocene dinoflagellate cyst biostratigraphy in the southern Andean foreland basin: Implications for drake passage throughflow, Andean Geol., 48, 185–218, https://doi.org/10.5027/andgeov48n2-3339, 2021b.

Brinkhuis, H.: Late Eocene to Early Oligocene dinoflagellate cysts from the Priabonian type-area (Northeast Italy); biostratigraphy and palaeoenvironmental interpretation, Palaeogeogr. Palaeocl., 107, 121–163, 1994.

Brinkhuis, H. and Schiøler, P.: Palynology of the Geulhemmerberg Cretaceous/Tertiary boundary section (Limburg, SE Netherlands), Geologie en Mijnbouw, 75, 193–213, 1996.

Brinkhuis, H., Bujak, J. P., Smit, J., Versteegh, G. J. M., and Visscher, H.: Dinoflagellate-based sea surface temperature reconstructions across the Cretaceous-Tertiary boundary, Palaeogeogr. Palaeocl., 141, 67–83, 1998.

Brinkhuis, H., Sengers, S., Sluijs, A., Warnaar, J., and Williams, G. L.: Latest Cretaceous to earliest Oligocene, and Quaternary dinoflagellate cysts from ODP Site 1172, East Tasman Plateau, in: Proceedings Ocean Drilling Program, Scientific Results, edited by: Exon, N. F., Kennett, J. P., and Malone, M., College Station, Texas, 1–48, https://doi.org/10.2973/odp.proc.sr.189.106.2003, 2003.

Brinkhuis, H., Schouten, S., Collinson, M. E., Sluijs, A., Sinninghe Damsté, J. S., Dickens, G. R., Huber, M., Cronin, T. M., Onodera, J., Takahashi, K., Bujak, J. P., Stein, R., van der Burgh, J., Eldrett, J. S., Harding, I. C., Lotter, A. F., Sangiorgi, F., van Konijnenburg-van Cittert, H., de Leeuw, J. W., Matthiessen, J., Backman, J., Moran, K., and the Expedition 302 Scientists: Episodic fresh surface waters in the Eocene Arctic Ocean, Nature, 441, 606–609, https://doi.org/10.1038/nature04692, 2006.

Bujak, J. P.: V. Dinoflagellate cysts and acritarchs from the Eocene of southern England, in: Bujak, J. P., Downie, C., Eaton, G. L., and Williams, G. L.: Dinoflagellate cysts and acritarchs from the Eocene of southern England, Special Papers in Palaeontology, no. 24, 100 p., pl. 1–22, 1980.

Bujak, J. P. and Brinkhuis, H.: Global warming and dinocyst changes across the Paleocene/Eocene Epoch boundary, in: Late Paleocene – early Eocene climatic and biotic events in the marine and terrestrial records, edited by: Aubry, M.-P., Lucas, S. G., and Berggren, W. A., Columbia University Press, New York, 277–295, ISBN 0-231-190238-0, 1998.

Bujak, J. P. and Mudge, D. C.: A high-resolution North Sea Eocene dinocyst zonation, Journal of the Geological Society, London, 151, 449–462, 1994.

Bujak, J. P., Downie, C., Eaton, G. L., and Williams, G. L.: Dinoflagellate cysts and acritarchs from the Eocene of southern England. Special Papers in Palaeontology, no. 24, 100 p., pl. 1–22, 1980.

Bütschli, O.: Protozoa, in: Klassen und Ordnungen des Thier-Reichs, Wissenschaftlich Dargestellt in Wort und Bild, edited by: Bronn, H. G., Wintersche Verlagsbuchhandling, Leibzig, 865–1088, 1885.

Casas-Gallego, M., Gogin, I., and Vieira, M.: Two new dinoflagellate cyst species and their biostratigraphical application in the Eocene and Oligocene of the North Sea, Palynology, 45, 337–349, https://doi.org/10.1080/01916122.2020.1819457, 2021.

Cookson, I. C. and Eisenack, A.: Some microplankton from the paleocene Rivernook Bed, Victoria, Proc. Roy. Soc. of Victoria, 80, 247–257, 1967.

Cramwinckel, M. J., Huber, M., Kocken, I. J., Agnini, C., Bijl, P. K., Bohaty, S. M., Frieling, J., Goldner, A., Hilgen, F. J., Kip, E. L.,

Peterse, F., van der Ploeg, R., Röhl, U., Schouten, S., and Sluijs, A.: Synchronous tropical and polar temperature evolution in the Eocene, Nature, 559, 382–386, https://doi.org/10.1038/s41586-018-0272-2, 2018.

Crouch, E. M. and Brinkhuis, H.: Environmental change across the Paleocene-Eocene transition from eastern New Zealand: A marine palynological approach, Mar. Micropaleontol., 56, 138–160, 2005.

Crouch, E. M., Heilmann-Clausen, C., Brinkhuis, H., Morgans, H. E. G., Rogers, K. M., Egger, H., and Schmitz, B.: Global dinoflagellate event associated with the late Paleocene thermal maximum, Geology, 29, 315–318, 2001.

Crouch, E. M., Brinkhuis, H., Visscher, H., Adatte, T., and Bolle, M.-P.: Late Paleocene- early Eocene dinoflagellate cyst records from the Tethys: Further observations on the global distribution of Apectodinium, in: Causes and Consequences of Globally Warm Climates in the Early Paleogene. Geological Society of America Special Paper 369, edited by: Wing, S. L., Gingerich, P. D., Schmitz, B., and Thomas, E., Geological Society of America, Boulder, Colorado, 113–131, 2003.

Crouch, E. M., Shepherd, C. L., Morgans, H. E. G., Naafs, B. D. A., Dallanave, E., Phillips, A., Hollis, C. J., and Pancost, R. D.: Climatic and environmental changes across the early Eocene climatic optimum at mid-Waipara River, Canterbury Basin, New Zealand, Earth-Sci. Rev., 200, 102961, https://doi.org/10.1016/j.earscirev.2019.102961, 2020.

Damassa, S. P.: Dinoflagellate cysts without walls: *Evittosphaerula paratabulata* Manum, 1979 and *Chaenosphaerula magnifica* gen. et sp. nov. from Deep Sea Drilling Project Site 338, Norwegian Sea, Rev. Palaeobot. Palyno., 98, 159–176, https://doi.org/10.1016/S0034-6667(97)00020-1, 1997.

Deflandre, G.: Considerations biologiques sur les microorganismes d'origine planctoniques conserves dans les silex de la craie, Bull. biol. France Belgique, 69, 213–244, 1935.

Denison, C. N.: Stratigraphic and sedimentological aspects of the worldwide distribution of *Apectodinium* in Paleocene/Eocene Thermal Maximum deposits, Geological Society, London, Special Publications, 511, 269–308, https://doi.org/10.1144/SP511-2020-46, 2021.

De Verteuil, L. and Norris, G.: Miocene dinoflagellate stratigraphy and systematics of Maryland and Virginia, Micropaleontology, 42 Supplement, 1–172, 1996.

Drugg, W. S.: Some New Genera, Species, and Combinations of Phytoplankton from the Lower Tertiary of the Gulf Coast, USA, Proceedings of the North American Paleontological Convention, 809–843, 1970.

Drugg, W. S. and Loeblich, A. R. J.: Some Eocene and Oligocene phytoplankton from the Gulf Coast, USA, Tulane Studies in Geology, 5, 181–194, 1967.

Eaton, G. L.: Dinoflagellate cysts from the Bracklesham Beds (Eocene) of the Isle of Wight, southern England, Bull. Brit. Mus (Nat. Hist.) Geol., 26, 227–332, 1976.

Edwards, L. E.: Miocene dinocysts from DSDP Leg 81, Rockall Plateau, eastern North Atlantic Ocean, in: Initial Reports of the Deep Sea Drilling Program 81, Washington, 581–594, https://doi.org/10.2973/dsdp.proc.81.114.1984, 1984.

Edwards, L. E.: Dinoflagellates from the Black Mingo Group (Paleocene) of South Carolina, T. Am. Philos. Soc., 88, 28–48, foi:10.2307/1006669, 1998.

Eisenack, A. and Gocht, H.: Neue Namen für einige Hystrichosphaeren der Bernsteinformation Ostpreussens, Neues Jahrb. Geol. P.-M., 511–581, 1960.

Eldrett, J. S. and Harding, I. C.: Palynological analyses of Eocene to Oligocene sediments from DSDP Site 338, Outer Vøring Plateau, Mar. Micropaleontol., 73, 226–240, https://doi.org/10.1016/j.marmicro.2009.10.004, 2009.

Evitt, W. R.: Sporopollenin dinoflagellate cysts: their morphology and interpretation, American Association of Stratigraphic Palynologists Foundation, Dallas, USA, 1985.

Fauconnier, D. and Masure, E.: Les dinoflagellés fossile. Guide pratique de détermination. Les genres à processus et à archéopyle apical, BRGM Editions, 2004.

Fensome, R. A., Taylor, F. J. R., Norris, G., Sarjeant, W. A. S., Wharton, D. I., and Williams, G. L.: A Classification of Fossil and Living Dinoflagellates, Micropaleontology, Special Publication, 351 pp., 1993.

Fensome, R. A., Williams, G. L., and MacRae, R. A.: The Lentin and Williams Index of Fossil Dinoflagellates, 2019 Edition, AASP Contributions Series Number 50, American Association of Stratigraphic Palynologists Foundation, 2019.

Fokkema, C. D., Agterhuis, T., Gerritsma, D., de Goeij, M., Liu, X., de Regt, P., Rice, A., Vennema, L., Agnini, C., Bijl, P. K., Frieling, J., Huber, M., Peterse, F., and Sluijs, A.: Polar amplification of orbital-scale climate variability in the early Eocene greenhouse world, Clim. Past, 20, 1303–1325, https://doi.org/10.5194/cp-20-1303-2024, 2024a.

Fokkema, C. D., Brinkhuis, H., Peterse, F., and Sluijs, A.: Orbital (Hydro)Climate Variability in the Ice-Free early Eocene Arctic, ESS Open Archive, Paleoceanogr. Paleocl., accepted, https://doi.org/10.22541/essoar.171259268.89696496/v1, 2024b.

Frieling, J. and Sluijs, A.: Towards quantitative environmental reconstructions from ancient non-analogue microfossil assemblages: Ecological preferences of Paleocene – Eocene dinoflagellates, Earth-Sci. Rev., 185, 956–973, https://doi.org/10.1016/j.earscirev.2018.08.014, 2018.

Frieling, J., Iakovleva, A. I., Reichart, G. J., Aleksandrova, G. N., Gnibidenko, Z. N., Schouten, S., and Sluijs, A.: Paleocene-Eocene warming and biotic response in the epicontinental West Siberian Sea, Geology, 42, 767–770, 2014.

Frieling, J., Huurdeman, E. P., Rem, C. C. M., Donders, T. H., Pross, J., Bohaty, S. M., Holdgate, G. R., Gallagher, S. J., McGowran, B., and Bijl, P. K.: Identification of the Paleocene–Eocene boundary in coastal strata in the Otway Basin, Victoria, Australia, J. Micropalaeontol., 37, 317–339, https://doi.org/10.5194/jm-37-317-2018, 2018a.

Frieling, J., Reichart, G.-J., Middelburg, J. J., Röhl, U., Westerhold, T., Bohaty, S. M., and Sluijs, A.: Tropical Atlantic climate and ecosystem regime shifts during the Paleocene–Eocene Thermal Maximum, Clim. Past, 14, 39–55, https://doi.org/10.5194/cp-14-39-2018, 2018b.

Gregory, W. A. and Hart, G. F.: Distribution of dinoflagellates in a subsurface marine Wilcox (Paleocene-eocene) section in southwest Louisiana, Palynology, 19, 45–75, https://doi.org/10.1080/01916122.1995.9989451, 1995.

Habib, D.: Neocomian dinoflagellate zonation in the western North Atlantic, Micropaleontology, 21, 373–392, 1975.

Harding, I. C., Charles, A. J., Marshall, J. E. A., Pälike, H., Roberts, A. P., Wilson, P. A., Jarvis, E., Thorne, R., Morris, E., Moremon, R., Pearce, R. B., and Akbari, S.: Sea-level and salinity fluctuations during the Paleocene-Eocene thermal maximum in Arctic Spitsbergen, Earth Planet. Sc. Lett., 303, 97–107, 2011.

Heilmann-Clausen, C.: Dinoflagellate stratigraphy of the Uppermost Danian to Ypresian in the Viborg 1 borehole, Central Jylland, Denmark, DGU A7, 1–69, https://doi.org/10.34194/seriea.v7.7026, 1985.

Hollis, C. J., Dunkley Jones, T., Anagnostou, E., Bijl, P. K., Cramwinckel, M. J., Cui, Y., Dickens, G. R., Edgar, K. M., Eley, Y., Evans, D., Foster, G. L., Frieling, J., Inglis, G. N., Kennedy, E. M., Kozdon, R., Lauretano, V., Lear, C. H., Littler, K., Lourens, L., Meckler, A. N., Naafs, B. D. A., Pälike, H., Pancost, R. D., Pearson, P. N., Röhl, U., Royer, D. L., Salzmann, U., Schubert, B. A., Seebeck, H., Sluijs, A., Speijer, R. P., Stassen, P., Tierney, J., Tripati, A., Wade, B., Westerhold, T., Witkowski, C., Zachos, J. C., Zhang, Y. G., Huber, M., and Lunt, D. J.: The DeepMIP contribution to PMIP4: methodologies for selection, compilation and analysis of latest Paleocene and early Eocene climate proxy data, incorporating version 0.1 of the DeepMIP database, Geosci. Model Dev., 12, 3149–3206, https://doi.org/10.5194/gmd-12-3149-2019, 2019.

Huber, M. and Caballero, R.: The early Eocene equable climate problem revisited, Clim. Past, 7, 603–633, https://doi.org/10.5194/cp-7-603-2011, 2011.

Iakovleva, A. I. and Heilmann-Clausen, C.: Early and middle Eocene dinoflagellate cysts from the Aktulagay section, Kazakhstan, Palynology, 45, 27–57, https://doi.org/10.1080/01916122.2019.1705933, 2021.

Iakovleva, A. I., Brinkhuis, H., and Cavagnetto, C.: Late Palaeocene-Early Eocene dinoflagellate cysts from the Turgay Strait, Kazakhstan; correlations across ancient seaways, Palaeogeogr. Palaeocl., 172, 243–268, 2001.

Jin, S., Kemp, D. B., Jolley, D. W., Vieira, M., Zachos, J. C., Huang, C., Li, M., and Chen, W.: Large-scale, astronomically paced sediment input to the North Sea Basin during the Paleocene Eocene Thermal Maximum, Earth Planet. Sc. Lett., 579, 117340, https://doi.org/10.1016/j.epsl.2021.117340, 2022.

Jolley, D., Vieira, M., Jin, S., and Kemp, D. B.: Palynofloras, palaeoenvironmental change and the inception of the Paleocene Eocene Thermal Maximum; the record of the Forties Fan, Sele Formation, North Sea Basin, J. Geol. Soc., 180, 2021–2131, https://doi.org/10.1144/jgs2021-131, 2023.

Kender, S., Stephenson, M. H., Riding, J. B., Leng, M. J., Knox, R. W. O. B., Peck, V. L., Kendrick, C. P., Ellis, M. A., Vane, C. H., and Jamieson, R.: Marine and terrestrial environmental changes in NW Europe preceding carbon release at the Paleocene–Eocene transition, Earth Planet. Sc. Lett., 353–354, 108–120, https://doi.org/10.1016/j.epsl.2012.08.011, 2012.

Klement, K. W.: Dinoflagellaten und Hystrichosphaerideen aus dem unteren und mittleren Malm Südwestdeutschlands, Palaeontographica, Abt. A., 114, 1–104, 1960.

Krishnan, S., Pagani, M., Huber, M., and Sluijs, A.: High latitude hydrological changes during the Eocene Thermal Maximum 2, Earth Planet. Sc. Lett., 404, 167–177, 2014.

Lentin, J. K. and Williams, G. L.: Fossil Dinoflagellates: Index to Genera and Species, 1977 Edition, Bedford Institute of Oceanography, Report Series, Bedford Institute of Oceanography, Dartmouth, NS, 209 pp., 1977.

Lentin, J. K. and Williams, G. L.: Fossil Dinoflagellates: Index to genera and species, 1993 Edition, in: AASP Contributions Series, 4, American Association of Stratigraphic Palynologists, 101–134, 1993.

Liengjarern, M., Costa, L., and Downie, C.: Dinoflagellate cysts from the Upper Eocene–Lower Oligocene of the Isle of Wight, Palaeontology, 23, 475–499, 1980.

Lindemann, E.: Abteilung Peridineae (Dinoflagellatae), in: Die Natürlichen Pflanzenfamilien nebst ihren Gattungen und wichtigeren Arten insbesondere den Nutzpflanzen. Zweite stark vermehrte und verbesserte Auflage herausgegeven von A. Engler. 2 Band, edited by: Engler, A. and Prantl, K., Wilhelm Engelmann, Leipzig, Germany, 3–104, 1928.

Manum, S. B.: Two new tertiary dinocyst genera from the norwegian sea: *Lophocysta* and *Evittosphaerula*, Rev. Palaeobot. Palyno., 28, 237–248, https://doi.org/10.1016/0034-6667(79)90026-5, 1979.

Marheinecke, U.: Monographie der Dinozysten, Acritarcha und Chlorophyta des Maastrichtium von Hemmoor (Niedersachsen), Palaeontogr. Abt. B, 227, 1–173, 1992.

März, C., Schnetger, B., and Brumsack, H. J.: Paleoenvironmental implications of Cenozoic sediments from the central Arctic Ocean (IODP Expedition 302) using inorganic geochemistry, Paleoceanography, 25, PA3206, https://doi.org/10.1029/2009pa001860, 2010.

März, C., Vogt, C., Schnetger, B., and Brumsack, H.-J.: Variable Eocene-Miocene sedimentation processes and bottom water redox conditions in the Central Arctic Ocean (IODP Expedition 302), Earth Planet. Sc. Lett., 310, 526–537, https://doi.org/10.1016/j.epsl.2011.08.025, 2011.

Morgan, R.: Some Early Cretaceous organic-walled microplankton from the Great Australian Basin, Australia J. and Proc. Roy. Soc. New South Wales, 108, 157–167, 1975.

Morgenroth, P.: Neue in organischer Substanz erhaltene Mikrofossilien des Oligozäns, Neues Jahrb. Geol. P.-A., 127, 1–12, 1966.

Mudie, P. J., Fensome, R. A., Rochon, A., and Bakrač, K.: The dinoflagellate cysts *Thalassiphora subreticulata* n.sp. and *Thalassiphora balcanica*: their taxonomy, ontogenetic variation and evolution, Palynology, 44, 237–269, https://doi.org/10.1080/01916122.2019.1567614, 2020.

Müller, R. D., Cannon, J., Qin, X., Watson, R. J., Gurnis, M., Williams, S., Pfaffelmoser, T., Seton, M., Russell, S. H. J., and Zahirovic, S.: GPlates: Building a Virtual Earth Through Deep Time, Geochem. Geophy. Geosy., 19, 2243–2261, https://doi.org/10.1029/2018gc007584, 2018.

Niechwedowicz, M.: Dinoflagellate cysts from the Upper Cretaceous (upper Campanian to lowermost Maastrichtian) of the Middle Vistula River section, Poland, Palynology, 46, 1–37, https://doi.org/10.1080/01916122.2021.1945700, 2022.

Nøhr-Hansen, H., Williams, G. L., and Fensome, R. A.: Biostratigraphic correlation of the western and eastern margins of the Labrador–Baffin Seaway and implications for the regional geology, GEUS Bulletin, 37, 1–74, https://doi.org/10.34194/geusb.v37.4356, 2016.

Norvick, M. S.: The microplankton genus *Disphaeria* Cookson and Eisenack emend, Bull. Austr. Bur. Min. Res, Geol & Geophys., 140, 45–46, 1973.

Pagani, M., Pedentchouk, N., Huber, M., Sluijs, A., Schouten, S., Brinkhuis, H., Sinninghe Damsté, J. S., Dickens, G. R., and Expedition 302 Scientists, T.: Arctic hydrology during global warming at the Palaeocene-Eocene thermal maximum, Nature, 442, 671–675, 2006.

Pascher, A.: Über Flagellaten und Algen, Deutsche Botanische Gesellachaft, Berichte, 32, 136–160, 1914.

Powell, A. J., Brinkhuis, H., and Bujak, J. P.: Upper Paleocene – Lower Eocene dinoflagellate cyst sequence biostratigraphy of southeast England, in: Correlation of the Early Paleogene in Northwest Europe, Geological Society Special Publication, 101, edited by: Knox, R. W. O. B., Corfield, R. M., and Dunay, R. S., 145–183, 1996.

Prasad, V., Uddandam, P. R., Agrawal, S., Bajpai, S., Singh, I., Mishra, A. K., Sharma, A., Kumar, M., and Verma, P.: Biostratigraphy, palaeoenvironment and sea level changes during pre-collisional (Palaeocene) phase of the Indian plate: palynological evidence from Akli Formation in Giral Lignite Mine, Barmer Basin, Rajasthan, Western India, International Union of Geological Sciences, 43, 476–488, https://doi.org/10.18814/epiiugs/2020/020030, 2020.

Premaor, E., Ferreira, E. P., Guerstein, G. R., and Souza, P. A.: Eocene paleoceanographic and paleoclimatic events recognized by assemblages of dinoflagellate cysts in the Southwest Atlantic Ocean, J. S. Am. Earth Sci., 130, 104587, https://doi.org/10.1016/j.jsames.2023.104587, 2023.

Pross, J. and Brinkhuis, H.: Organic-walled dinoflagellate cysts as paleoenvironmental indicators in the Paleogene; a synopsis of concepts, Palaeont. Z., 79, 53–59, 2005.

Pross, J. and Schmiedl, G.: Early Oligocene dinoflagellate cysts from the Upper Rhine Graben (SW Germany): Paleoenvironmental and paleoclimatic implications, Mar. Micropaleontol., 45, 1–24, 2002.

Prothero, D. R. and Schwab, F.: Sedimentary Geology (2nd Edition), Freeman and Company, New York, 557 pp., ISBN 0716739054, 9780716739050, 2004.

Rush, W., Self-Trail, J., Zhang, Y., Sluijs, A., Brinkhuis, H., Zachos, J., Ogg, J. G., and Robinson, M.: Assessing environmental change associated with early Eocene hyperthermals in the Atlantic Coastal Plain, USA, Clim. Past, 19, 1677–1698, https://doi.org/10.5194/cp-19-1677-2023, 2023.

Sangiorgi, F., van Soelen, E. E., Spofforth, D. J. A., Pälike, H., Stickley, C. E., St. John, K., Koç, N., Schouten, S., Sinninghe Damsté, J. S., and Brinkhuis, H.: Cyclicity in the middle Eocene central Arctic Ocean sediment record: Orbital forcing and environmental response, Paleoceanography, 23, PA1S08, https://doi.org/10.1029/2007PA001487, 2008.

Schiøler, P.: Dinoflagellate cysts and acritarchs from the Oligocene–Lower Miocene interval of the Alma-1X well, Danish North Sea, J. Micropalaeontol., 24, 1–37, https://doi.org/10.1144/jm.24.1.1, 2005.

Schreck, M., Meheust, M., Stein, R., and Matthiessen, J.: Response of marine palynomorphs to Neogene climate cooling in the Iceland Sea (ODP Hole 907A), Mar. Micropaleontol., 101, 49–67, https://doi.org/10.1016/j.marmicro.2013.03.003, 2013.

Seton, M., Müller, R. D., Zahirovic, S., Gaina, C., Torsvik, T., Shephard, G., Talsma, A., Gurnis, M., Turner, M., Maus, S., and Chandler, M.: Global continental and ocean basin reconstructions since 200Ma, Earth-Sci. Rev., 113, 212–270, https://doi.org/10.1016/j.earscirev.2012.03.002, 2012.

Sluijs, A. and Brinkhuis, H.: A dynamic climate and ecosystem state during the Paleocene-Eocene Thermal Maximum: inferences from dinoflagellate cyst assemblages on the New Jersey Shelf, Biogeosciences, 6, 1755–1781, https://doi.org/10.5194/bg-6-1755-2009, 2009.

Sluijs, A. and Brinkhuis, H.: High Arctic late Paleocene and early Eocene dinoflagellate cysts; dinocyst results from IODP Expedition 302 (ACEX), Zenodo [data set], https://doi.org/10.5281/zenodo.10998746, 2024.

Sluijs, A. and Dickens, G. R.: Assessing offsets between the $\delta^{13}C$ of sedimentary components and the global exogenic carbon pool across Early Paleogene carbon cycle perturbations, Global Biogeochem. Cy., 26, GB4005, https://doi.org/10.1029/2011GB004224, 2012.

Sluijs, A., Pross, J., and Brinkhuis, H.: From greenhouse to icehouse; organic-walled dinoflagellate cysts as paleoenvironmental indicators in the Paleogene, Earth-Sci. Rev., 68, 281–315, 2005.

Sluijs, A., Schouten, S., Pagani, M., Woltering, M., Brinkhuis, H., Sinninghe Damsté, J. S., Dickens, G. R., Huber, M., Reichart, G.-J., Stein, R., Matthiessen, J., Lourens, L. J., Pedentchouk, N., Backman, J., Moran, K., and the Expedition 302 Scientists: Subtropical Arctic Ocean temperatures during the Palaeocene/Eocene thermal maximum, Nature, 441, 610–613, 2006.

Sluijs, A., Brinkhuis, H., Schouten, S., Bohaty, S. M., John, C. M., Zachos, J. C., Reichart, G.-J., Sinninghe Damsté, J. S., Crouch, E. M., and Dickens, G. R.: Environmental precursors to light carbon input at the Paleocene/Eocene boundary, Nature, 450, 1218–1221, 2007.

Sluijs, A., Brinkhuis, H., Crouch, E. M., John, C. M., Handley, L., Munsterman, D., Bohaty, S., M., Zachos, J. C., Reichart, G.-J., Schouten, S., Pancost, R. D., Sinninghe Damsté, J. S., Welters, N. L. D., Lotter, A. F., and Dickens, G. R.: Eustatic variations during the Paleocene-Eocene greenhouse world, Paleoceanography, 23, PA4216, https://doi.org/10.1029/2008PA001615, 2008a.

Sluijs, A., Röhl, U., Schouten, S., Brumsack, H.-J., Sangiorgi, F., Sinninghe Damsté, J. S., and Brinkhuis, H.: Arctic late Paleocene–early Eocene paleoenvironments with special emphasis on the Paleocene-Eocene thermal maximum (Lomonosov Ridge, Integrated Ocean Drilling Program Expedition 302), Paleoceanography, 23, PA1S11, https://doi.org/10.1029/2007PA001495, 2008b.

Sluijs, A., Schouten, S., Donders, T. H., Schoon, P. L., Röhl, U., Reichart, G. J., Sangiorgi, F., Kim, J.-H., Sinninghe Damsté, J. S., and Brinkhuis, H.: Warm and Wet Conditions in the Arctic Region during Eocene Thermal Maximum 2, Nat. Geosci., 2, 777–780, 2009.

Sluijs, A., Bijl, P. K., Schouten, S., Röhl, U., Reichart, G.-J., and Brinkhuis, H.: Southern ocean warming, sea level and hydrological change during the Paleocene-Eocene thermal maximum, Clim. Past, 7, 47–61, https://doi.org/10.5194/cp-7-47-2011, 2011.

Sluijs, A., Frieling, J., Inglis, G. N., Nierop, K. G. J., Peterse, F., Sangiorgi, F., and Schouten, S.: Late Paleocene–early Eocene Arctic Ocean sea surface temperatures: reassessing biomarker paleothermometry at Lomonosov Ridge, Clim. Past, 16, 2381–2400, https://doi.org/10.5194/cp-16-2381-2020, 2020.

Speelman, E. N., Sewall, J. O., Noone, D., Huber, M., von der Heydt, A., Sinninghe Damsté, J. S., and Reichart, G.-J.: Modeling the influence of a reduced equator-to-pole sea surface temperature gradient on the distribution of water isotopes in the Early/Middle Eocene, Earth Planet. Sc. Lett., 298, 57–65, https://doi.org/10.1016/j.epsl.2010.07.026, 2010.

Steeman, T., De Weirdt, J., Smith, T., De Putter, T., Mees, F., and Louwye, S.: Dinoflagellate cyst biostratigraphy and palaeoecology of the early Paleogene Landana reference section, Cabinda Province, Angola, Palynology, 44, 280–309, https://doi.org/10.1080/01916122.2019.1575091, 2020.

Stein, R., Boucsein, B., and Meyer, H.: Anoxia and high primary production in the Paleogene central Arctic Ocean: First detailed records from Lomonosov Ridge, Geophys. Res. Lett., 33, L18606, https://doi.org/10.1029/2006GL026776, 2006.

Stockmarr, J.: Tablets with spores used in absolute pollen analysis, Pollen et Spores, 13, 615–621, 1972.

Stover, L. E. and Evitt, W. R.: Analyses of Pre-Pleistocene organic-walled Dinoflagellates, Geological Sciences, Stanford University Publications, Stanford, 300 pp., 1978.

Stover, L. E. and Hardenbol, J.: Dinoflagellates and depositional sequences in the Lower Oligocene (Rupelian) Boom clay formation, Belgium, Bulletin van de Belgische Vereniging voor Geologie/Bulletin de la Societe belge de Geologie, T., 102, 5–77, 1994.

Taylor, F. J. R.: On dinoflagellate evolution, BioSystems, 13, 65–108, 1980.

Thöle, L. M., Nooteboom, P. D., Hou, S., Wang, R., Nie, S., Michel, E., Sauermilch, I., Marret, F., Sangiorgi, F., and Bijl, P. K.: An expanded database of Southern Hemisphere surface sediment dinoflagellate cyst assemblages and their oceanographic affinities, J. Micropalaeontol., 42, 35–56, https://doi.org/10.5194/jm-42-35-2023, 2023.

Torsvik, T. H., Van der Voo, R., Preeden, U., Mac Niocaill, C., Steinberger, B., Doubrovine, P. V., van Hinsbergen, D. J. J., Domeier, M., Gaina, C., Tohver, E., Meert, J. G., McCausland, P. J. A., and Cocks, L. R. M.: Phanerozoic polar wander, palaeogeography and dynamics, Earth-Sci. Rev., 114, 325–368, https://doi.org/10.1016/j.earscirev.2012.06.007, 2012.

Vieira, M. and Jolley, D.: Stratigraphic and spatial distribution of palynomorphs in deep-water turbidites: A meta-data study from the UK central North Sea paleogene, Mar. Petrol. Geol., 122, 104638, https://doi.org/10.1016/j.marpetgeo.2020.104638, 2020.

Vieira, M., Mahdi, S., Casas-Gallego, M., and Fenton, J.: Three new Paleocene dinoflagellate cysts from the North Sea and the Norwegian Sea, Rev. Palaeobot. Palyno., 258, 256–264, https://doi.org/10.1016/j.revpalbo.2018.09.002, 2018.

Vieira, M., Mahdi, S., and Holmes, N.: High resolution biostratigraphic zonation for the UK central North Sea Paleocene, Mar. Petro. Geol., 117, 104400, https://doi.org/10.1016/j.marpetgeo.2020.104400, 2020.

Waddell, L. M. and Moore, T. C.: Salinity of the Eocene Arctic Ocean from Oxygen Isotope Analysis of Fish Bone Carbonate, Paleoceanography, 23, PA1S12, https://doi.org/10.1029/2007PA001451, 2008.

Wall, D., Dale, B., Lohmann, G. P., and Smith, W. K.: The environmental and climatic distribution of dinoflagellate cysts in modern marine sediments from regions in the North and South Atlantic Oceans and adjacent seas, Mar. Micropaleontol., 2, 121–200, 1977.

Willard, D. A., Donders, T. H., Reichgelt, T., Greenwood, D. R., Sangiorgi, F., Peterse, F., Nierop, K. G. J., Frieling, J., Schouten, S., and Sluijs, A.: Arctic vegetation, temperature, and hydrology during Early Eocene transient global warming events, Global Planet. Change, 178, 139–152, https://doi.org/10.1016/j.gloplacha.2019.04.012, 2019.

Williams, G. L. and Downie, C.: Further dinoflagellate cysts from the London Clay, in: Studies on Mesozoic and Cainozoic dinoflagellate cysts. Bulletin of the British Museum (Natural History) Geology 3, edited by: Davey, R. J., Downie, C., Sarjeant, W. A. S., and Williams, G. L., 215–248, 1966.

Williams, G. L., Brinkhuis, H., Pearce, M. A., Fensome, R. A., and Weegink, J. W.: Southern Ocean and global dinoflagellate cyst events compared; index events for the Late Cretaceous-Neogene, in: Proceedings Ocean Drilling Program, Scientific Results, 189, edited by: Exon, N. F., Kennett, J. P., and Malone, M. J., College Station, Texas, 1–98, https://doi.org/10.2973/odp.proc.sr.189.107.2004, 2004.

Williams, G. L., Fensome, R. A., and MacRae, R. A.: The Lentin and Williams Index of Fossil Dinoflagellates, 2017 Edition, AASP Contributions Series Number 48, American Association of Stratigraphic Palynologists Foundation, 2017.

Zonneveld, K. A. F., Marret, F., Versteegh, G. J. M., Bogus, K., Bonnet, S., Bouimetarhan, I., Crouch, E., de Vernal, A., Elshanawany, R., Edwards, L., Esper, O., Forke, S., Grøsfjeld, K., Henry, M., Holzwarth, U., Kielt, J.-F., Kim, S.-Y., Ladouceur, S., Ledu, D., Chen, L., Limoges, A., Londeix, L., Lu, S. H., Mahmoud, M. S., Marino, G., Matsouka, K., Matthiessen, J., Mildenhal, D. C., Mudie, P., Neil, H. L., Pospelova, V., Qi, Y., Radi, T., Richerol, T., Rochon, A., Sangiorgi, F., Solignac, S., Turon, J.-L., Verleye, T., Wang, Y., Wang, Z., and Young, M.: Atlas of modern dinoflagellate cyst distribution based on 2405 data points, Rev. Palaeobot. Palyno., 191, 1–197, https://doi.org/10.1016/j.revpalbo.2012.08.003, 2013.